Delay Compensation in Bilateral Teleoperation Using Predictor Observers

by

Tuğba Leblebici

Submitted to the Graduate School of Sabancı University
in partial fulfillment of the requirements for the degree of
Master of Science

Sabancı University

August, 2010

Delay Compensation in Bilateral Teleoperation Using Predictor Observers

APPROVED BY:

Assoc. Prof. Dr. Mustafa Ünel
(Thesis Advisor) ....

Prof. Dr. Asif Şabanoviç ....

Assist. Prof. Dr. Ahmet Onat ....

Assist. Prof. Dr. Kürşat Şendur ....

Assoc. Prof. Dr. Erkay Savaş ....

DATE OF APPROVAL: ....

Delay Compensation in Bilateral Teleoperation Using Predictor Observers

Tuğba Leblebici

ME, Master's Thesis, 2010

Thesis Supervisor: Assoc. Prof. Mustafa Ünel

Keywords: Bilateral teleoperation, communication delay, predictor observer, disturbance observer, four channel controller

Abstract

Destabilization and performance degradation problems caused by the time delay in communication channel is a serious problem in bilateral teleoperation. In particular, variability of the delay due to limited bandwidth, long distance or congestion in transmission problems has been a real challenge in bilateral teleoperation research since the internet communication has become prevalent. Many existing delay compensation techniques are designed for linear teleoperator systems. In order to implement them on real bilateral systems, the nonlinear dynamics of the robots must first be linearized. For this purpose feedback linearization is usually employed.

In this thesis, the delay compensation problem is tackled in an observer framework by designing two observers. Integration of a disturbance observer to the slave side implies a linearized slave dynamics with nominal parameters. Disturbance observer estimates the total disturbance (nonlinear terms, parametric uncertainties and external disturbances) on the slave system. A second observer is designed at the master side to predict states of the slave. This observer can be designed using a variety of linear or nonlinear methods.

In order to have finite-time convergence, a sliding mode observer is designed at the master side. It is shown that this observer predicts the future positions and/or velocities of the slave and use of such predictions in the computation of a simple PD control law implies stable operation for the bilateral system. Since the disturbance observer increases the robustness of the slave system, the performance of the resulting bilateral system is quite satisfactory.

Force reflecting bilateral teleoperation is also considered in this thesis. Integrating the proposed observer based delay compensation technique into the well known four-channel control architecture not only stable but also transparent bilateral teleoperation is achieved. Simulations with bilateral systems consisting of 2 DOF scara robots and pantograph robots, and experiments with bilateral systems consisting of a pair of single link robots and a pair of pantograph robots validate the proposed method.

İki Yönlü Sistemlerde Yordayıcı Gözlemciler Kullanarak Gecikme Telafisi

Tuğba Leblebici

ME, Master Tezi, 2010

Tez Danışmanı: Doç. Dr. Mustafa Ünel

Anahtar Kelimeler: İki yönlü teleoperasyon, iletişim gecikmesi, yordayıcı gözlemci, bozucu gözlemcisi, dört kanallı denetleyici

Özet

İletişim kanalındaki gecikmeden kaynaklanan kararsızlaşma ve performans düşüklüğü, iki yönlü teleoperasyonda karşılaşılan oldukça zor problemlerdir. Özellikle, internet kullanımının yaygınlaşmasıyla sınırlı bant genişliğinden, uzun mesafelerden ya da iletim sırasında oluşan yığılmadan kaynaklanan değişken gecikme problemi bilateral teleoperasyon araştırmalarında çözülmesi beklenen önemli bir problem haline gelmiştir. Mevcut gecikme telafisi yöntemlerinin çoğu doğrusal teleoperatör sistemleri için tasarlanmıştır. Bunları gerçek iki yönlü sistemlere uygulamak için öncelikle robotun doğrusal olmayan dinamiği doğrusallaştırılmalıdır. Geribeslemeyle doğrusallaştırma yöntemi bu amaç için sıkça kullanılan bir yöntemdir. Bu tezde, gecikme telafisi problemi, gözlemci çerçevesinde ele alınmıştır. Bu amaçla iki yeni gözlemci tasarlanmıştır. Bozucu gözlemci, yönetilen sistem üzerindeki toplam bozucu etkiyi (doğrusal olmayan terimler, parametre belirsizlikleri ve dış bozucular) tahmin eder. Bozucu gözlemcinin yönetilen sistem tarafına entegre edilmesi, nominal parametrelerle ifade edilen doğrusallaştırılmış bir yönetilen sistem dinamiği oluşturur. Bir başka gözlemci ise yöneten sistem tarafında yönetilen sistemin durum değişkenlerini tahmin etmek üzere tasarlanmıştır. Bu gözlemci, doğrusal ve doğrusal olmayan çeşitli yöntemlerle tasarlanabilir. Sonlu zaman yakınsaması sağlayabilmek için yöneten sistem tarafında bir kayan kipli gözlemci tasarlanmıştır. Bu gözlemcinin yönetilen sistemin gelecekteki pozisyonlarını ve/veya hızlarını tahmin ettiği ve bu tahminlerin basit bir PD denetleyicisinde kullanılarak kararlı bir operasyon sağladığı gösterilmiştir. Bozucu gözlemci sistemin gürbüzlüğünü artırdığından, ortaya çıkan iki yönlü sistemin performansı yeterli düzeydedir.

Bu tezde kuvvet yansımalı iki yönlü teleoperasyon da ele alınmıştır. Önerilen gözlemci tabanlı gecikme telafisi tekniği iyi bilinen dört-kanallı kontrol mimarisine entegre edilerek sadece kararlı değil aynı zamanda saydam bir teleoperasyon sağlanmıştır. Önerilen yöntem, 2 serbeslik dereceli scara robotlar ve pantograf robotlardan oluşan bilateral sistemlerde yapılan simulasyonlar ve tek eksenli bir robot çifti ve pantograf çiftinden oluşan iki yönlü sistemlerde yapılan başarılı deney sonuçları ile doğrulanmıştır.

Acknowledgements

It is a great pleasure to extend my gratitude to my thesis advisor Assoc. Prof. Dr. Mustafa Ünel for his precious guidance and support. I am greatly indebted to him for his supervision and excellent advises throughout my Master study.

I would like to thank Prof. Dr. Asıf Şabanoviç, Assist. Prof. Dr. Ahmet Onat, Assist. Prof. Kürşat Şendur and Assoc. Prof. Dr. Erkay Savaş for their feedbacks and spending their valuable time to serve as my jurors.

I would like to acknowledge the financial support provided by TUBITAK (The Scientific and Technological Research Council of Turkey) through the project "Bilateral teleoperation systems with time delay" under the grant 106M533.

I would sincerely like to thank to bilateral teleoperation project members Duruhan Özçelik and Serhat Dikyar for their pleasant team-work and providing me the necessary motivation during hard times.

Many thanks to Melda Şener, Çağrı Gürbüz, Kaan Taha Öner, Ahmet Can Erdoğan, Sena Ergüllü, Yusuf Sipahi, Efe Sırımoğlu, Cevdet Hançer, Ozan Tokatlı, Aykut Cihan Satıcı, Alper Ergin and all mechatronics laboratory members I wish I had the space to acknowledge in person, for their great friendship throughout my Master study.

Finally, I would like to thank my family for all their love and support throughout my life.

Contents

List of Figures

List of Tables

Chapter I

1 Introduction

Bilateral teleoperation has been a highly challenging problem in robotics circles in recent decades. Teleoperation and telepresence are two concepts that should be considered together in bilateral teleoperation. Teleoperation is defined as operating a remote system from a distance and telepresence is the virtual existence of a manipulator in a distant location. An operator can perform a task that is impossible even for autonomous robots or work in hazardous and unsanitary environments as if he/she is present there. Space-based applications or underwater robotics are examples to applications performed in such environments. Telesurgery which enables a surgeon to operate a surgery even from another continent is a very popular application of bilateral teleoperation.

Bilateral teleoperation structure is composed of a human operator, local system, communication channel, remote system and environment. Position, velocity or force information is shared between the local and remote sides through the communication channel. A human operator can control a remote system by utilizing the information he/she gets from the remote system. Local and remote systems are generally called master and slave respectively. Reference signals like position, velocity or force are generated at the master side and sent to the remote side through the communication channel.

Likewise, force information is generated at the slave side as the slave robot contacts with the environment and this information is sent to the master side through the channel. Thus the human operator feels the environment force (transperancy) as if he is in the remote side (telepresence). It is said the operator is kinesthetically coupled with the environment.

The major problem in bilateral teleoperation is the existence of delay and data loss in the communication channel. The signals transmitted through the channel in forward and reverse directions are incurred to constant or time variable delay and due to the delay, stability and transparency cannot be achieved in bilateral teleoperation systems. In order to tackle the stability problem, numerous approaches are proposed and developed in the literature since the work of Sheridan and Ferrell [1]. The authors worked on remote manipulation and performed experiments to observe the completion time of simple tasks. They concluded that, the destabilizing effect of delay could be eliminated by a strategy called move and wait strategy. Sheridan and Ferrell didn't use force reflection in their experiments. As force feedback was first used in [2], [3], it was shown experimentally that when feedback signals are used in bilateral teleoperation, delays on the order of tenth of a second yields the system unstable. Stability could only be obtained for the references with very small bandwidth. Communication delay caused nonlinearities and increase of the system dimension to infinity, thus there was little work in literature in those years. Leung et. al. and Lin et. al. performed analysis on destabilizing effects of delay on bilateral control systems in later years [4], [5].

As a breakthrough, Anderson and Spong proposed a passivity based method to address the stability problem in bilateral teleoperation [6]. By using passivity theory and defining the scattering operator, they proved that the communication channel cannot sustain its passivity in the existence of time delay. Scattering transformation is utilized to introduce lossless transmission line and provide passivity of the system regardless of bandwidth. Stability of the method was proven only intuitively in [6] but asymptotic stability was proven analytically in 1989 [7].

While performing some tasks such as micro-surgery, micro or macro manipulation and micro assembly, the mismatch of the signals at master and slave sides motivated the idea of scaled telemanipulation. Colgate proposed an impedance scaling technique in Laplace domain [8] and Kosuge proposed the same idea in time domain [9]. Both of the methods are based on the passivity theory.

In 1991, Niemeyer and Slotine reformulated the scattering theory and introduced new variables called wave variables [10]. In this context the power flow at the input and output of the communication channel is redefined as input and output waves. Wave variables are obtained by applying the wave transformation to the velocity and force signals (power signals) before they enter the communication channel. The same results, as in the scattering theory, were obtained by wave theory. In wave variables technique, wave reflections are observed at junctions and terminations when the impedance of the wave carriers change. By matching the characteristic impedance of the wave transmission to the remaining system, wave reflections could be avoided. The stability of the system was proven by passivity theory but since the performance of the method was not satisfactory performance improvement studies continued. In [11], transient behavior of the bilateral system is analyzed and a tuning mechanism is developed to make adjustments between the telepresence and operation speed.

Since the internet is started to be used in the middle of 1990's, the communication delay problem was turned into time variable communication delay problem. In internet communication, the delay becomes variable due to factors like bandwidth, congestion and distance. Packet losses and reordering of data is also observed. The effect of time variable delay and packet losses in packet switched network is investigated by Hirche and Buss [12]. Oboe and Fiorini also studied on internet based teleoperation and performed experiments in order to examine the effect of time variable delay on stability of the system [13],[14]. In 1998, a bilateral teleoperation environment was specifically designed for studying time variable internet delays. The behavior of the delay was observed with this system and a control method which is utilized from delay parameters was proposed [15]. In 2002, Lozano, Chopra and Spong handled the time variable delay problem and showed that the time variable delay destabilizes the system by rendering it nonpassive [16],[17]. The authors modified the scattering transformation method and guaranteed passivity of the system under variable time delay by introducing a time variable gain into the communication block.

As the internet technology has highly developed and internet based teleoperation gained more attention, wave variables based approaches are also extended. Systems with unpredictable time variable delay was studied in [18] where wave variable filters were used to preserve the stability. For the purpose of obtaining explicit position feedback and avoiding numerical integration step, instead of wave variables, wave integrals were transmitted through the communication channel. Chopra, Bestesky and Spong also studied on the extension of passivity based methods for internet communication [19].

They suggested to add two Communication Management Modules which were responsible for reconstructing scattering variables. This method guarantee passivity and asymptotic stability of the system when variable time delay exists in the communication channel.

Passivity based methods can be considered as the fundamental approaches that motivate the delay compensation problem in bilateral teleoperation. Although asymptotic stability was proven and velocity convergence was provided, exact position tracking could not be maintained in earlier passivity based studies. The wave matching method was able to suppress the oscillations, however tracking errors in position and force tracking could not be compensated. In 2001 position tracking errors were eliminated by removing one of the matching elements (from master side) and exact force reflections (transparency) were satisfied in the existence of variable delay in communication channel [20]. In this method impedance parameter 'b' was used to compensate the variations of time delay by changing it as a function of the delay to keep the gain margin constant. In order to tackle the position convergence problem, Chopra et al. extended the wave variable based approach by adding a term proportional to the delayed position error in both master and slave sides and achieved better position tracking [21], [22]. In their Kalman filter based method, Munir and Book studied the position drift problem in 2004 [23]. Another passivity based architecture for handling force and position tracking problem in delay compensation of bilateral teleoperation was proposed by Namerikawa and Kawada in 2006 [24]. In the method, the impedances of the local and remote sides are matched by adding virtual damping to the both sides. Establishing position control gains by Lyapunov stability based methods, possible deteriorations on the operation ability of the system due to the virtual damping can be avoided.

In 2005, Lee and Spong, proposed a PD based control method for teleoperation systems consisting of multi DOF nonlinear robots under a constant communication time delay [25]. In the previous passivity based methods, the passivity of the teleoperation system blocks were provided individually. As an improvement, in this method, the closed loop teleoperation system was passified as a whole. Position convergence that had implicitly been provided in earlier scattering approaches, was ensured exponentially. In this work the communication delay was considered to be the same in forward and backward directions (symmetric) and known exactly. In 2006 Lee and Spong removed this unrealistic ideas and considered the delay as unknown and asymmetric [26]. They used controller passivity concept, the Lyapunov-Krasovskii technique and Parseval's identity for passifying the communication and control blocks together. Nuno et al. claimed in their paper ([27]) that, since any L_∞ stable mapping from velocity to force cannot be defined, the assumptions which Lee and Spong used in their approach were unverifiable. Nuno and his colleagues proved that, with the injection of sufficiently large damping to both manipulator subsystems makes the subsystems passive and this yields stable behavior of nonlinear teleoperators with PD like control structure. They controlled the teleoperators with either delayed force or delayed position error. As the velocities converge to zero (if the human and environment forces are bounded), position coordination is achieved by adding gravity compensation. Thus, it was shown that, without passivity and scattering transformation, PD-like structures could control bilateral systems under constant delay and the approach in [26] was also proven. In this paper, it was also referred that the idea of damping injection may degrade performance. In [28], authors developed simple P-like and PD-like position controllers which provide global position tracking for nonlinear teleoperators under variable time delay. Stability of the bilateral system has been proven by a Lyapunov analysis. Position and velocity convergence is achieved if any external force is not applied on either of the master or slave systems.

Andriot et al. presented a synthesis method to design a generalized bilateral control based on the passivity theory [29]. They considered the delay problem for flexible and rigid joint manipulators and claimed that the problem was completely solved for rigid manipulators. For the flexible joint manipulators, H_∞ based control method was suggested. In telerobotics, H_∞ control theory is used by Kazerooni and Tsay [30],[31]. Dynamic behavior of master and slave systems were defined to be functions of each other. H_∞ control theory and model reduction technique was used to guarantee that the system behavior was governed by the proposed specified functions. Instead of velocity and position information, force information was transferred between the two systems but force transfer required wider bandwidth between the master and slave. Position tracking error occurred because of not transferring velocity or position information. In these studies free motion of slave was not considered, only contact motion was considered. Although the proposed methods provided stability, degradation of performance due to the communication delay could not be avoided. In 1995, a new approach was developed by using H_∞ control and μ analysis and synthesis technique [4]. Unlike the previous methods, this method considered the performance and stability against communication delay together. Again in this work, the control method was designed for both environment contact and free motion cases. In this method, constant and upper bounded delay was considered as a perturbation to the constrained motion (contact with the environment) and this perturbation was filtered to have norm less than 1. Then μ synthesis method was applied to the system to design the controller. In 1998 Sano designed controllers for several values of bounded delay and with the use of gain scheduling, he selected the suitable controller for the measured delay. This was a suitable idea for Internet based teleoperation [32].

An alternative bilateral system with dynamic environment where the system is incurred to time variable delay was proposed by Kikuchi, Tekeo and Kosuge [33]. The proposed system is a combination of three subsystems which are bilateral teleoperation, visual information and environment predictive display subsystems. The camera system at the slave side was collecting pictures and sending them to the master system. Because of the variable communication delay, the information sent through the visual information subsystem could not be used for bilateral teleoperation. Therefore, environment predictive display subsystem which provided the estimated current position of the slave manipulator and the environment was used.

A modified sliding mode controller based time variable delay compensation method was proposed in 1999 [34]. In this method, an impedance controller was used at the master side while a sliding mode controller was used at the slave side. In this method, the nonlinear sliding mode control gain didn't depend on the delay variations, thus the amount of delay didn't need to be known and the controller gains could be tuned independent of the delay.

Prediction based methods also took place in the literature of delay compensation methods. Smith predictor is one of these methods which is based on elimination of delay terms from the characteristic equation of the control systems [35], [36]. Munir and Book derived a predictor from a modified Smith predictor along with Kalman filter [37],[38]. An energy regulator was used in this method to provide passivity. Wave variables and Smith predictor methods were combined by Ganjefar, Momeni and Janabi in 2002 [39]. A paper covering predictive control methods proposed a neural network and Smith predictor based predictive controller method [40].

Natori, Tsuji, Ohnishi proposed Communication Disturbance Observer method (CDOB) for the compensation of variable communication delay. Unlike predictor based methods, in this method it was not necessary to know the amount of delay so that it could be applied to the systems under time variable delay. In this method the effect of delay was considered as external disturbance force acting on the communication channel and this disturbance force was eliminated by communication disturbance observer [41]-[43]. However the eliminated force was not only the disturbance force, it also included the environmental force in the case of contact with the environment. For this reason, force information couldn't be transferred to the master side precisely. In 2009 $CDOB$ method was extended so that the environmental force was separated from the communication disturbance [44]- [46]. In [45] external forces are calculated by reaction torque/force estimation observer (RTOB). RTOB is designed as a kind of disturbance observer that uses position information to estimate the reaction forces acting on a system [47]. In order to provide transparent teleoperation, Ohnishi and his colleagues used four channel controller method in which force and velocity signals are transmitted in both directions. This control architecture was proposed by Lawrence in 1992 and by Yokokohji and Yoshikawa in 1994 independently [48], [49], [50]. In order to provide a perfect transparency between master and slave systems, the impedance seen by the human operator should be equal to the impedance of the environment. By using the two-port *hybrid parameter matrix*, Lawrence showed that transparency cannot be achieved without using four information channels. Yokokohji also addressed the same idea by using the *chained matrix*. In the conventional method, the four channel controller was designed to control the system in position mode. In 1995, Zhu and Salcudean improved Lawrence's formalism so that transparency could also be provided for the systems that operate in velocity (rate) control mode [51]. Unlike Lawrence's method, force sensing is not required in [52]. Estimate of the environment impedance is used to obtain the contact information. In the mentioned four channel controller based approaches, it is assumed that master, slave, environment and operator impedances are perfectly known. In order to circumvent the uncertainty problems adaptive control based schemes came forward. Zaad and Salcudean developed an adaptive control method where force feedback is not used [53]. Adaptation on both sides of the teleoperator is considered in [54].

Wave variables method is also improved for force reflecting teleoperators [55], [56]. In [57], an additional wave impedance in the wave variable transformation is implemented in order to provide the transparency of the bilateral teleoperation system.

1.1 Motivation

Bilateral teleoperation allows a human operator to manipulate a slave system located at a certain distance remotely via a master system and interact with the remote environment at the same time (Fig. 1.1). A closed loop interaction is necessary for the successful achievement of these two goals.

Control, reference or feedback signals are transmitted through a communication channel from master to slave and from slave to master sides. Possible communication delays in the channel may cause not only unstability but also degradation in the performance of the task realization. In force reflecting teleoperation, the environment cannot be perceived due to the communication delay. Stability and performance issues have been a real challenge in the field of bilateral teleoperation and numerous researchers have contributed to this field over the last decades. The developments on communication and robotics technology necessitated improvements on the existing delay compensation techniques. The common use of internet required extensions on the delay compensation techniques for variable communication delay.

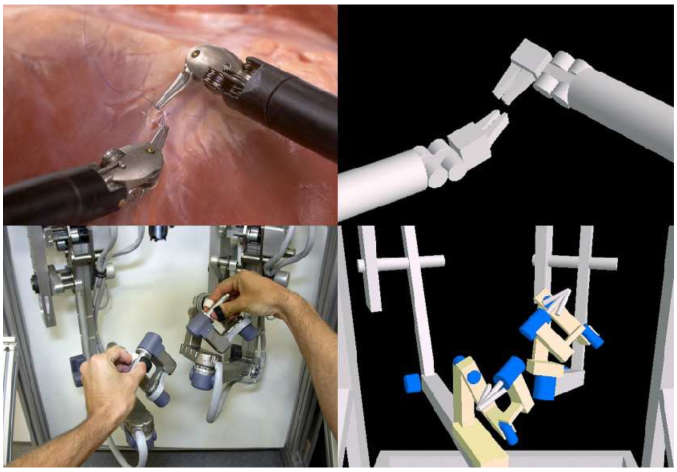

Figure 1.1: Remote surgery

In bilateral teleoperation studies, mostly linear and single degree of freedom systems are considered as master and slave manipulators for simplicity until today. However, more complicated systems such as nonlinear multi degree of freedom robots are being used in robotics applications recently. As the complexity and the nonlinearity of the system increases, modeling uncertainties appear in addition to parametric uncertainties and system nonlinearities. Stability in bilateral teleoperation could be attained by designing controllers considering the system nonlinearities or linearizing the system dynamics.

1.2 Thesis Contributions and Organization

In this thesis, a novel observer based time delay compensation method for nonlinear bilateral teleoperator systems is proposed. It consists of two types of observers: disturbance observers (DOB) at both master and slave sides which render nonlinear dynamics of the master and slave robots linear, and a sliding mode observer (SMO) at the master side which predicts the future states (position and velocity) of the slave. Any system can be transformed into a nominal one by eliminating the undesired terms from the model of the system. Undesired terms may be external disturbances acting on the system like viscous friction, coulomb friction and gravity or internal disturbances like modeling uncertainties, parameter uncertainties and nonlinear terms. Estimation of the nonlinear terms or other disturbances are rendered by disturbance observer. Extracting the estimated nonlinear terms from the system dynamics, a nonlinear system can be linearized.

Utilization of disturbance observer implies a linear system with nominal parameters which in turn allows application of the predictor observer. Predictor observer approach is based on using the states of an observer that mimics the behavior of nominal slave system in control calculations. The precise estimation of the actual system states is possible with accurate measurement of available states. The predictor observer SMO is composed of a two-step structure. In the first step, the finite-time convergence of the measured system states incurred to communication delay to intermediate observer states is provided by sliding mode control approach. The equivalent control generated in first step is used in second step for the convergence of estimated states to actual states.

Unlike many other teleoperation schemes where position or velocity of the master is sent to the slave side as reference, in the observer based approach the control signal for the slave is computed at the master side and sent through the communication medium. Slave's position (and/or velocity) is in turn sent to the master side through the same medium. Delayed signals sent from the slave side are used in the construction of the SMO observer at the master side.

Contact with environment condition is considered in bilateral force reflecting teleoperation framework. The control of the system is provided by four channel controller structure that is developed in an early study of Lawrence [48]. The control method is used together with predictor sliding mode observer to compensate communication delay in bilateral teleoperation systems where environment contact possibly occurs.

Proposed approach is verified with several simulations on Matlab/Simulink and experiments performed on a pair of pantograph robots where time delay is artificially created with Matlab's Time-Variable Delay block. Control algorithms are implemented in realtime using dSpace1103 controller board.

The contributions of the thesis can be summarized as follows:

- A novel observer based time delay compensation method for nonlinear bilateral teleoperator systems is proposed. Nominal linear teleoperators are obtained by employing disturbance observers and communication delay is compensated by a predictor observer.

- The control input for the slave manipulator is designed at the master side using the estimated states of the slave system and sent to the remote side.

- Telepresence is provided by using a four channel control architecture so that unknown environment conditions are handled in control of the system.

- As nonlinear teleoperator systems, 2 DOF pantograph robots are designed and produced. Several experiments are performed in real time using dSpace1103 controller board.

The thesis is organized as follows: Section II describes modeling of linear and nonlinear bilateral systems with time delay, explains delay compensation methods that take important part in the literature and explains the four channel control architecture that is used in force reflecting bilateral teleoperation. Section III presents design of predictor observers and disturbance observers. Section IV describes force reflecting bilateral teleoperation and modified predictor observer designed for such teleoperation. Section V presents and discusses simulation and experimental results of constant and time variable delay compensation on various platforms working in master-slave configuration. Finally, Section VI concludes the thesis with some remarks and indicates possible future directions.

1.3 Notes

This thesis work is developed in the context of a TUBITAK (The Scientific and Technological Research Council of Turkey) and NSF (National Science Foundation) funded joint research project under the grant 106M533.

The following publications are produced from this thesis:

Journal Articles

- Delay Compensation in Bilateral Control Using Predictor Sliding Mode Observers, T. Leblebici, B. Çallı, M. Ünel, A. Şabanoviç, S. Bogosyan, M. Gökaşan, Turkish Journal of Electrical Engineering and Computer Sciences (TJEECS), 2011.

Conference Proceedings

- Delay Compensation for Nonlinear Teleoperators Using Predictor Observers, S. Dikyar, T. Leblebici, D. Özçelik, M. Ünel, A. Şabanoviç, S. Bogosyan, IEEE International Conference on Industrial Electronics, Control and Instrumentation (IECON 2010), November 7-10, Glendale, AZ, USA

- Doğrusal Olmayan İki Yönlü Denetim Sistemlerinde Gözlemci Tabanlı Zaman Gecikme Telafisi, T. Leblebici, S. Dikyar, D. Özçelik, M. Ünel, A. Şabanoviç, TOK'10: Otomatik Kontrol Ulusal Toplantısı, Gebze Yüksek Teknoloji Enstitüsü, Kocaeli, Turkey, 21-23 Eylül 2010,

- İki Yönlü Denetimde İletişim Kanalındaki Gecikmenin Kayan Kipli Gözlemci Kullanarak Telafisi, B. Çallı, T. Leblebici, M. Ünel, A. Şabanoviç, S. Bogosyan, M. Gökaşan, TOK'09: Otomatik Kontrol Ulusal Toplantısı, İstanbul Teknik Üniversitesi, İstanbul, Turkey, 13-16 Ekim 2009.

Chapter II

2 Bilateral Teleoperation

Bilateral teleoperation is based on the idea that the signals generated at both the master and slave systems are shared between each other in two directions. In bilateral teleoperation a remote manipulator could only be controlled by a human operator provided that the force/torque references that is imposed to a local manipulator are transmitted to the remote side precisely. For accurate realization of the task, the environmental factors that may possibly affect the task performance should be perceived by the human operator. As the force is applied on the master manipulator, this results in the motion of the master and position reference to be tracked by the slave is generated. On the other hand if the slave manipulator contacts with environment at the remote side, force/torque information which restricts the motion of the slave is generated. Sharing the generated signals at both sides through the communication channel allows slave manipulator to track the master's position and human operator to perceive the remote environment. This operation enables the operator to execute a task somewhere without actually being there.

A bilateral system can be stabilized by a simple PD controller and a successful performance of position tracking is achieved if there is no delay in the communication channel. On the other hand, even a very small amount of delay (e.g. $0.05 - 0.1$ sec) can degrade the performance and finally makes the system unstable. A simple stability analysis shows that as time delay increases, poles of the transfer function of the closed-loop system move toward the right hand complex plane and turns the system into an unstable one. In the following subsections, modeling of linear and nonlinear bilateral teleoperation systems will be explained, fundamental methods that exist in the literature for providing stability against communication delay are presented.

2.1 Modeling of Bilateral Teleoperation Systems

A bilateral teleoperation system is usually composed of a human operator, a master system, communication channel, a slave system and the environment (Fig. 2.1). In the literature different bilateral control architectures are proposed based on the type of shared signals (position, velocity and force). In some of these systems, master's velocity is sent to the slave side while force measured at slave side is sent to the master side (Fig. 2.2).

Figure 2.1: Bilateral Teleoperation System

In observer based approaches, however, the control input (force or torque) for the slave is computed at the master side and sent to the slave side while position (and/or velocity) of the slave is fed back to the master side and used in control calculations as shown in Fig. 2.3.

According to the complexity of the task, linear or nonlinear systems are used as master and slave manipulators in bilateral teleoperation. Even

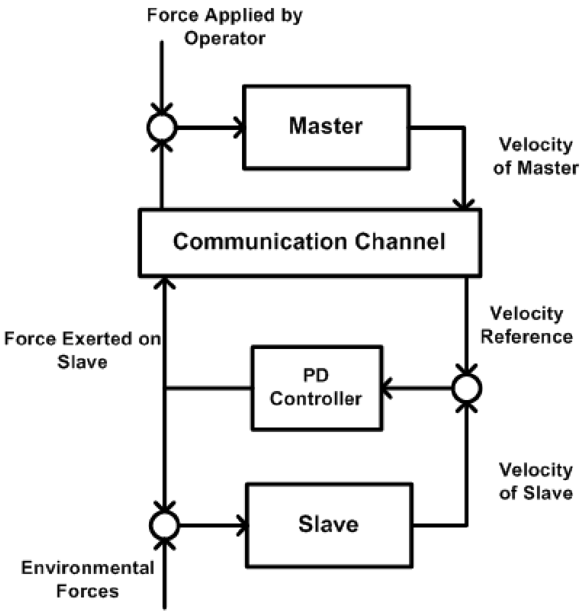

Figure 2.2: Bilateral Control architecture where velocity and force information are shared.

though the nonlinear systems are difficult to be analyzed, applying linearization techniques renders the control of such systems possible. Modeling of linear and nonlinear teleoperators is explained in the following two subsections.

2.1.1 Linear Teleoperators

In order to simplify the analysis of bilateral systems, usually 1 DOF bilateral control systems are employed in discussions. In such systems, slave is a 1 DOF robot arm and its dynamics is modeled as

$$J_s\ddot{q}_s(t) + b_s\dot{q}_s(t) = \tau_s(t) + \tau_{ds} \tag{2.1}$$

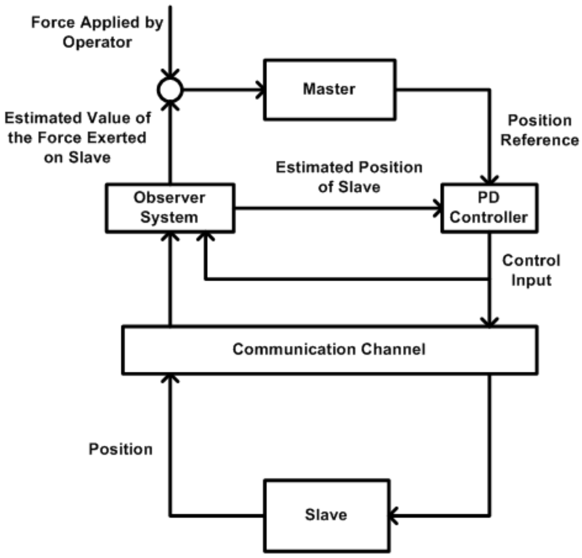

Figure 2.3: Bilateral control architecture where control input and position information are shared.

In this equation J_s, b_s, $\ddot{q}_s$, $\dot{q}_s$, represent moment of inertia, damping coefficient, angular acceleration and angular velocity of the robot arm, respectively. Input torque which is the difference between the motor torque and the environmental torque and external disturbances acting on the slave system are represented by τ_s and τ_{ds} respectively. Likewise, master robot which is manipulated by a human operator can be described similarly as

$$J_m\ddot{q}_m(t) + b_m\dot{q}_m(t) = \tau_m(t) + \tau_{dm} \tag{2.2}$$

where subscript m emphasizes the fact that related quantities belong to the master robot. τ_m is net input torque defined as the difference between the torque applied by the operator and the torque generated by the motor. External disturbances acting on the master system is represented by τ_{dm}.

2.1.2 Nonlinear Teleoperators

Performing some tasks are only possible with manipulators that has nonlinear dynamics having multiple degrees of freedom. In order to analyze such systems, a n DOF bilateral control system is employed in discussions. In such a system, slave is a n DOF robot arm and its dynamics is modeled as

$$\tau_s = D_s(q_s)\ddot{q}_s + C_s(q_s, \dot{q}_s)\dot{q}_s + F_{Gs}(q_s) + B_s\dot{q}_s + \tau_{ds} \tag{2.3}$$

where q_s is the vector of joint angles, $D_s(q_s)$ is the $n \times n$ positive-definite inertia matrix, $C_s(q_s, \dot{q}_s)$ is the $n{\times}n$ Coriolis-centripetal matrix, $F_{Gs}(q_s)$ is the $n \times 1$ gravitational force vector, B_s is the viscous friction (damping) matrix and τ_{ds} is an external disturbance vector. Input torque vector which is the difference between the manipulator torque and the environmental torque is represented by τ_s. Likewise, master robot which is manipulated by a human operator can be described similarly as

$$\tau_m{=}D_m(q_m)\ddot{q}_m + C_m(q_m, \dot{q}_m)\dot{q}_m + F_{Gm}(q_m) + B_m\dot{q}_m + \tau_{dm} \tag{2.4}$$

where subscript m emphasizes the fact that related quantities belong to the master robot. τ_m is net input torque vector defined as the difference between the torque applied by the operator and the torque generated by the manipulator.

2.2 Scattering Transformation Approach

Stability of bilateral control systems under time delay could not be achieved in a serious theoretical framework until the seminal work by Anderson and Spong in 1989 [6]. In this work, authors attributed instability of the system to the non-passive nature of the communication channel. In order to analyze a system in the context of passivity the power entering to the system should be defined first. It is defined as the scalar product between the input vector (x) and the output vector (y) of the system. In addition, a lower-bounded energy storage function E and a non-negative power dissipation function P_{diss} are also defined. With these definitions a system is said to be passive, if it obeys:

$$P = x^T y = \frac{dE}{dt} + P_{diss} \tag{2.5}$$

which means the power is either stored in the system or dissipated. This implies that the total energy supplied by the system up to time t is limited to the initial stored energy i.e. the energy transfer is lower bounded by the negative initial energy:

$$\int_0^t P\, d\tau = \int_0^t x^T y\, d\tau = E(t) - E(0) + \int_0^t P_{diss}\, d\tau \geq -E(0) = constant. \tag{2.6}$$

Anderson and Spong proposed so called *scattering transformation* which renders the communication channel passive and proved that for any constant delay the passivity of the system can be preserved by using scattering transformation. Scattering theory analyzes the stability problem considering it in the context of transmission line. Effort and flow (voltage and current in this case) are transmitted without losing energy and without changing the steady-state behavior of the signal through the communication channel when the ideal lossless transmission line is provided. Stability of the system is affected by the line impedance Z_o, environment impedance Z_e and human impedance Z_h. In frequency domain, a linear $2-$port lossless communication line element is defined as

$$\begin{aligned} F_h(s) &= Z_o tanh(\tfrac{sL}{V_o})V_m(s) + sech(\tfrac{sL}{V_o})F_e(s) \\ -V_s(s) &= -sech(\tfrac{sL}{V_o})V_m(s) + (tanh(\tfrac{sL}{V_o})/Z_o)F_e(s) \end{aligned} \tag{2.7}$$

where $Z_o = \sqrt{\frac{L}{C}}$, $V_o = \frac{1}{LC}$, L is the characteristic inductance, C is the capacitance for the transmission line, $F_h(s)$ and $F_e(s)$ are the Laplace transformation of human and environment forces respectively and similarly $V_m(s)$ and $V_s(s)$ are the master and slave velocities expressed in Laplace domain.

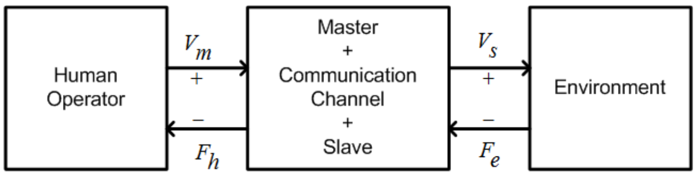

Figure 2.4: 2−Port Model of Teleoperation Systems

If the teleoperation system is established as shown in Fig. 2.4 the relationship between the forces and velocities in bilateral teleoperation can be characterized for LTI systems by the *Hybrid matrix* ($H(s)$ in Laplace domain) which is defined as follows:

$$\begin{bmatrix} F_h(s) \\ -V_s(s) \end{bmatrix} = \underbrace{\begin{bmatrix} h_{11}(s) & h_{12}(s) \\ h_{21}(s) & h_{22}(s) \end{bmatrix}}_{\triangleq H(s)} \begin{bmatrix} V_m \\ F_e \end{bmatrix} \tag{2.8}$$

For an ideal one degree of freedom teleoperation system, the ideal hybrid matrix that provides transparent teleoperation is

$$H_{ideal}(s) = \begin{bmatrix} 0 & 1 \\ -1 & 0 \end{bmatrix}$$

The scattering operator, S, which is mapping the input and output flow of the $2-$port network block is defined as $(F-V) = S(F+V)$ and it can be written as the scattering matrix for multi DOF systems in Laplace domain as $(F(s)-V(s)) = S(s)(F(s)+V(s))$. The scattering matrix can be written in terms of hybrid matrix as

$$S(s) = \begin{bmatrix} 1 & 0 \\ 0 & -1 \end{bmatrix} [H(s) - I][H(s) + I]^{-1}$$

Using the scattering matrix, passivity is proven by the following theorem:

Theorem 2.1. *A system is passive if and only if the norm of the scattering operator is less than or equal to one ($\|S\| \leqslant 1$)*

However if T amount of constant communication delay is imposed on the system then the hybrid and the scattering matrices become as

$$H(s) = \begin{bmatrix} 0 & e^{-sT} \\ -e^{-sT} & 0 \end{bmatrix}$$

and

$$S(s) = \begin{bmatrix} -tanh(sT) & sech(sT) \\ sech(sT) & tanh(sT) \end{bmatrix}$$

which makes the norm of the scattering matrix unbounded and yields the system non-passive and unstable. In order to provide the stability of the system the teleoperation system should be rendered passive. Passive system is obtained by providing the transmission line lossless i.e. setting $Z_o = 1$ and

$V_o = L/T$. Then the transmission line equations become as

$$\begin{aligned} F_h(s) &= Z_o tanh(sT)V_m(s) + sech(sT)F_e(s) \\ -V_s(s) &= -sech(sT)V_m(s) + tanh(sT)F_e(s) \end{aligned} \tag{2.9}$$

then the scattering matrix which satisfy the passivity condition with $\|S\| = 1$ is given by

$$S(s) = \begin{bmatrix} 0 & e^{sT} \\ e^{sT} & 0 \end{bmatrix}$$

2.3 Wave Variables Approach

In 1991 Niemeyer and Slotine reformulated the scattering theory and defined new variables called wave variables [10]. Wave variables represent the input and output power flow at each side of the communication channel as input and output waves. Wave transformation is applied on the velocity and force signals (power signals) before they enter the communication channel and the signals are transformed into wave variables. Damping is injected into the communication channel and stability has been proven in the "passivity" framework.

In order to define the wave variables, the power flow is first defined as

$$P = \dot{x}^T F = \frac{1}{2}u^T u - \frac{1}{2}v^T v \tag{2.10}$$

where F is the force (effort) and $\dot{x}$ is the velocity (flow) and they can be represented by any other effort and flow pair. In wave variables technique $\frac{1}{2}u^T u$ and $\frac{1}{2}v^T v$ specifies the power flow along and against a main direction respectively. The first and the second terms of P are components with positive and negative values respectively. The wave variables (u,v) can be computed from the standard power variables (x, F) by the following transformation.

$$\begin{aligned} u_m(t) &= 1/\sqrt{2b}(F_m + b\dot{x}_m(t)) \\ v_s(t) &= 1/\sqrt{2b}(F_s + b\dot{x}_s(t)) \end{aligned} \tag{2.11}$$

where u_m and v_s represent the forward and backward moving waves respectively and b is the characteristic wave impedance that may be a positive constant or a symmetric positive matrix. The power to wave variables transformation is shown in Fig. 2.5.

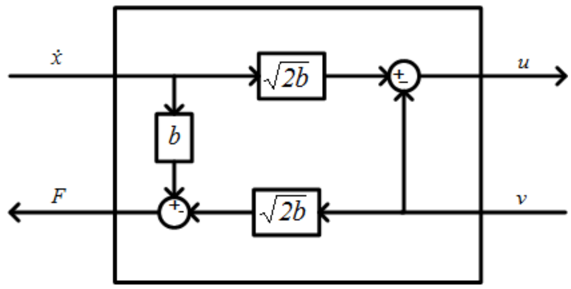

Figure 2.5: Transformation of power variables into wave variables

As the signals are transmitted along the communication channel with time delay, they are obtained as

$$\begin{aligned} u_s(t) &= u_{m_d}(t) = u_m(t-T) \\ v_m(t) &= v_{s_d}(t) = v_s(t-T) \end{aligned} \tag{2.12}$$

The overall system structure is shown in Fig. 2.6

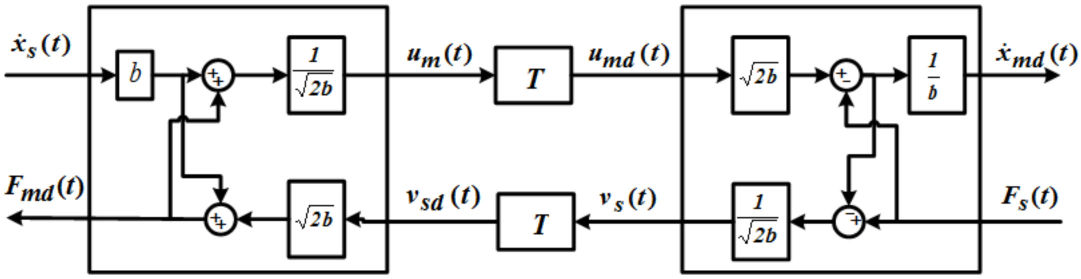

Figure 2.6: Wave variables

Applying the following transformations

$$\begin{aligned}
\dot{x}_s(t) &= \sqrt{\tfrac{2}{b}}u_s(t) + \tfrac{1}{b}F_s(t) \\
F_s(t) &= -b\dot{x}_s(t) + \sqrt{2b}u_s(t) \\
\dot{x}_m(t) &= \sqrt{\tfrac{2}{b}}v_m(t) + \tfrac{1}{b}F_m(t) \\
F_m(t) &= b\dot{x}_m(t) - \sqrt{2b}v_m(t)
\end{aligned} \tag{2.13}$$

the power input can be defined by the wave variables as

$$P_{in} = \frac{1}{2}u_m^T u_m - \frac{1}{2}v_m^T v_m - \frac{1}{2}u_s^T u_s + \frac{1}{2}v_s^T v_s \tag{2.14}$$

By substituting the terms in (2.12) into (2.14) and integrating, we obtain

$$P_{in} = \frac{d}{dt}[\int_{t-T}^{t} \frac{1}{2}u_m(\tau)^2\, d\tau + \frac{1}{2}u_s(\tau)^2\, d\tau] \tag{2.15}$$

Therefore this is a lossless passive communication with a positive energy storage function which simply integrates the power of the waves for the duration of the transmission. In particular, its passivity property is completely independent of the actual time delay. We obtain a lossless transmission line since the wave variables approach implicitly yields Eqn. (2.7). Then, we can conclude that the wave variables transformation provides a scattering transformation. The overall structure of the system is as shown in the figure below

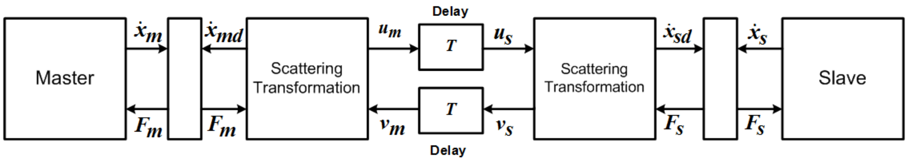

Figure 2.7: Bilateral teleoperation with scattering transformation

2.4 Lyapunov Based Approaches

In the literature, scattering and wave variables techniques are used for a long time to cope with the destabilizing effects of time delay in bilateral communication. With the approach proposed in 2005 by Lee and Spong, PD based control schemes are started to gain prevalence. In these modified proportional or proportional-derivative controller methods the passivity is basically provided by the addition of a dissipation gain to passify the teleoperation system. By injecting sufficiently large damping to both manipulator systems, unstability problem of nonlinear teleoperators could also be tackled. It is proven that transmitted signals are bounded and velocity signals belong to $\mathcal{L}_2$ space. Furthermore, with this method velocities converge to zero if the forces applied by the human and the environment are bounded.

According to the Proposition 2 in [27], the P-like controller is given by the following equations

$$\begin{aligned} \tau_m &= K_m(q_s(t - T_s(t)) - q_m) - B_m\dot{q}_m \\ \tau_s &= K_s(q_s - q_m(t - T_m(t))) - B_s\dot{q}_s \end{aligned} \tag{2.16}$$

where B_i are the damping coefficients of the master and slave systems respectively $(i = m, s)$, variable delays T_i are upper bounded by ${}^*T_i(t)$ and the control gains K_i are set such that

$$4B_m B_s > ({}^*T_m^2 + {}^*T_s^2) K_m K_s \tag{2.17}$$

which implies the velocities and position error bounded. Moreover if the system does not interact with the human or environment, position convergence is obtained by asymptotic convergence of the velocities to zero. The block diagram of bilateral teleoperation structure with P-like controller is shown in Fig. 2.8

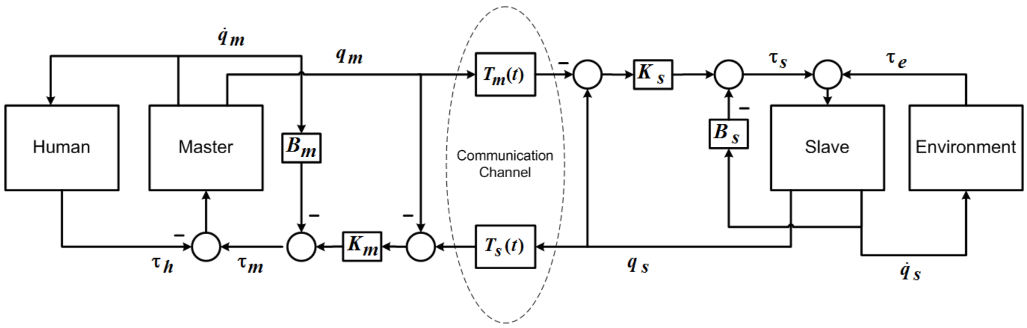

Figure 2.8: P-like controller

In the same context another controller namely PD-like controller is described as

$$\begin{aligned} \tau_m &= K_d(\gamma_s \dot{q}_s(t - T_s(t)) - \dot{q}_m) + K_m(q_s(t - T_s(t)) - q_m) - B_m \dot{q}_m \\ \tau_s &= K_d(\dot{q}_s - \gamma_m \dot{q}_m(t - T_m(t))) + K_s(q_m(t - T_m(t)) - q_s) - B_s \dot{q}_s \end{aligned} \tag{2.18}$$

where $\gamma_i = \sqrt{1 - \dot{T}_i}$. As it can be observed from the Lyapunov function given in the stability proof of the controller, the time varying gains (γ_i) dissipate the energy generated in the communication channel. PD-like controller block diagram is given in Fig. 2.9

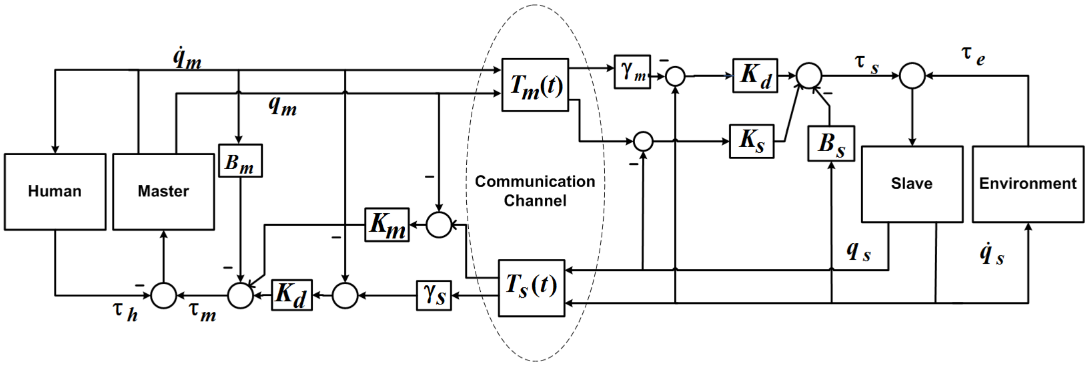

Figure 2.9: PD-like controller

2.5 Four Channel Controller Architecture

Stable manipulation and transparency are the two main goals in bilateral control architecture design. Transparency is achieved provided that the transmitted impedance is matched with the environment impedance ($Z_t = Z_e$) or the following conditions are satisfied:

$$x_m = x_s$$
$$F_h = -F_e$$

which means the slave tracks the master position precisely and the environment force is perceived by the human operator. On the other hand, for a stable teleoperation, the passivity of the system should be achieved by passivity theory. According to the passivity theory, if the subsystems (master, slave, communication channel, environment and human) are passive, then the interconnected bilateral teleoperation system is also passive. Several different stability and transparency techniques exist in the literature. Variety of the signals transmitted through the communication channel is one of the factors that designate the control system architecture. The number of virtual channels used for the interconnection between master and slave is another classification scheme. In the literature, two, three and four channel architectures have been proposed for stable force reflecting teleoperation. In this thesis four channel control architecture where the forces and velocities are transmitted in both ways is used. In Fig. 2.10 the master and slave dynamics are represented by the impedances Z_m and Z_s respectively. Similarly, C_m and C_s represent the master and slave controllers and $C_1 - C_4$ blocks denote the velocity and force controllers in forward and backward directions.

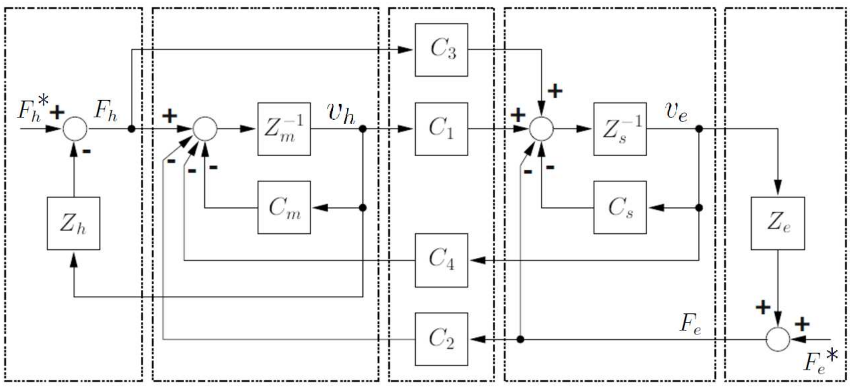

Figure 2.10: Block diagram of a four channel bilateral teleoperation system

The overall force reflecting bilateral teleoperation system can be defined by the Eqn. (2.8) using the hybrid matrix, which was previously defined in section 2.2. The parameters of the hybrid matrix are calculated by solving the Eqn. (2.8) and they are defined in terms of the subsystems of the bilateral system designed based on four-channel control structure as

$$
\begin{aligned}
h_{11} &= (Z_m + C_m)D(Z_s + C_s - C_3C_4) + C_4 \\
h_{12} &= -(Z_m + C_m)D(I - C_3C_2) - C_2 \\
h_{21} &= D(Z_s + C_s - C_3C_4) \\
h_{22} &= -D(I - C_3C_2)
\end{aligned}
\tag{2.19}
$$

where $D = (C_1 + C_3Z_m + C_3C_m)^{-1}$. The ideal hybrid matrix that yields the perfect transperancy was also defined in section 2.2. In order to satisfy the ideal condition of the hybrid matrix, the control parameters $C_1 - C_4$ should be chosen as

$$
\begin{aligned}
C_1 &= Z_s + C_s \\
C_2 &= I \\
C_3 &= I \\
C_4 &= -(Z_m + C_m)
\end{aligned}
\tag{2.20}
$$

where acceleration measurements are required to design the master and slave controllers C_m and C_s since the master and slave impedances contain 's' terms ([48],[64],[65]). A method to avoid this problems is proposed in [54] providing the perfect transperancy by designing the controllers as $C_1 = C_s$, and $C_4 = -C_m$.

Lawrence concluded the conflicting characteristics of transperancy and stability since using the four channel architecture yields more transparent teleoperation however on the contrary it increases destabilization of the system.

Chapter III

3 An Observer Based Approach to Communication Delay Problem

In observer based approaches presented in the literature, control input of the slave is computed at master side and transmitted to the slave side through the communication channel. Position or velocity of slave is fed back to the master side through the same channel (Fig. 2.3 and Fig. 3.1).

Figure 3.1: Sharing control input and position signals in observer based teleoperation systems

The observer or predictor based delay compensation methods in the literature are originated by Smith predictor in the late $1950's$ [66]. By assuming that the communication delay is constant and known, a Smith predictor provides a prediction of the nondelayed output of the plant [66]. In the Smith predictor approach, the plant model is utilized and the delay is moved out of the control loop. However, since the delay is uncertain and variable in internet communication, performance of the model based approach deteriorates. In this thesis a predictor based method is designed where the amount of delay is not necessary to be known.

3.1 Predictor Sliding Mode Observers

An observer that predicts the states of the slave is designed in the master side. The predictor observer is designed over a nominal slave model that is also obtained by disturbance observers in the master and slave sides.

A linear slave dynamics can be expressed by the following scalar differential equations in state-space:

$$\begin{aligned} \dot{p}(t) &= \omega(t) \\ J_s\dot{\omega}(t) + b_s\omega(t) &= \tau_s(t) \end{aligned} \tag{3.1}$$

Suppose the time delays from master to slave and from slave to master are denoted by T_1 and T_2, respectively, and they are constant. The input to the slave robot will be $\tau_s = u(t - T_1)$ assuming no interaction between the slave and the environment. On the other hand, the position of the slave will reach to the master side as $p_d(t) = p(t-T_2)$(see Fig. 3.1). Since the equation block (3.1) can be defined for all t, substituting t with $t - T_2$ in the equation, it can be rewritten as

$$\begin{aligned} \dot{p}(t-T_2) &= \omega(t-T_2) \\ J_s\dot{\omega}(t-T_2) + b_s\omega(t-T_2) &= \tau_s(t-T_2) \end{aligned} \tag{3.2}$$

Since $p_d(t) = p(t - T_2)$, $w_d(t) = w(t - T_2)$ and $\tau_s(t - T_2) = u(t - T_2 - T_1) = u(t - (T_2 - T_1)) = u(t - T)$, then the slave dynamics in terms of the delayed signals can be written as

$$\begin{aligned} \dot{p}_d(t) &= \omega_d(t) \\ J_s\dot{\omega}_d(t) + b_s\omega_d(t) &= u(t-T) \end{aligned} \tag{3.3}$$

where $T = T_1 + T_2$ represents the total round-trip delay that the system is incurred to.

3.1.1 Sliding Mode Observer

In order to predict position (and/or velocity) of the slave system, we construct the following sliding mode observer (SMO):

$$\dot{\hat{p}}(t) = \hat{\omega}(t) \tag{3.4}$$

$$J_s\dot{\hat{\omega}}(t) + b_s\omega_e(t) = u(t) + u_o(t) \tag{3.5}$$

$$J_s\dot{\omega}_e(t) = J_s\dot{\omega}_d(t) - u_{oeq}(t) \tag{3.6}$$

$$\dot{p}_e(t) = \omega_e(t) \tag{3.7}$$

where $\hat{p}$ and $\hat{\omega}$ are observer's intermediate variables and p_e and ω_e are estimated angular position and velocity of the slave. SMO input and its equivalent part are denoted as u_o and u_{oeq}. The observer is called Sliding Mode Observer since it is designed in the framework of sliding mode control. As it will be shown analytically, observer's intermediate variables ($\hat{p}(t)$, $\hat{\omega}(t)$) are pushed to position and velocity signals that reach to the master side with delay while the estimated variables (p_e,w_e) are pushed to the future position and velocity values of the slave.

In order to design the observer input, an observer error is defined as the difference between the delayed position $p_d(t)$ and the intermediate variable $\hat{p}(t)$, as

$$e(t) = p_d(t) - \hat{p}(t) \tag{3.8}$$

The first and second derivatives of the observer error are written as below:

$$\dot{e}(t) = \omega_d(t) - \hat{\omega}(t) \tag{3.9}$$

$$\ddot{e}(t) = \dot{\omega}_d(t) - \dot{\hat{\omega}}(t) \tag{3.10}$$

Substituting $\dot{\hat{\omega}}(t)$ from Eqn 3.5 into the second derivative yields

$$\ddot{e}(t) = \dot{\omega}_d(t) + \frac{b_s}{J_s}\omega_e(t) - \frac{u(t)}{J_s} - \frac{u_o(t)}{J_s} \tag{3.11}$$

Since the observer input will be designed in SMC (sliding mode control) framework, a sliding surface is defined in terms of observer error as

$$\sigma = \dot{e}(t) + Ce(t) \tag{3.12}$$

where $C > 0$ is the slope of the sliding surface. In sliding mode control (SMC) theory, the control that keeps the system on the sliding surface is called *equivalent control*. Since $\sigma = 0$ when the system is on the sliding surface, equivalent control can be computed by setting $\dot{\sigma}$ to zero. Substituting error and its derivative into Eqn. (3.12), $\dot{\sigma}$ is obtained as

$$\dot{\sigma} = \dot{\omega}_d(t) + \frac{b_s}{J_s}\omega_e(t) - \frac{1}{J_s}u(t) - \frac{1}{J_s}u_o(t) + C\dot{e}(t) \tag{3.13}$$

By setting $\dot{\sigma}$ to zero, we get the so-called equivalent control

$$u_{oeq}(t) = J_s\dot{\omega}_d(t) + b_s\omega_e(t) - u(t) + J_sC\dot{e}(t) \tag{3.14}$$

Observer input is the sum of the equivalent control $u_{oeq}(t)$ and a discontinuous term ($Ksgn(\sigma)$). Hence, we have

$$u_o(t) = u_{oeq}(t) - Ksgn(\sigma) \tag{3.15}$$

where $K > 0$ is a gain parameter and $sgn(.)$ denotes the well-known signum function. It is straightforward through a Lyapunov analysis to show that the control law given in (3.15) can transfer the system onto the sliding surface in finite time from arbitrary initial conditions in state-space and stabilizes there.

Lemma 1. *The observer defined by the equations in (3.4)-(3.7) predicts the future position (and/or velocity) of the slave system.*

Proof. Substituting the equivalent control given by (3.14) into (3.6) implies

$$J_s\dot{\omega}_e(t) = -b_s\omega_e(t) + u(t) - J_sC\dot{e}(t) \tag{3.16}$$

Replacing t by $t + T$ in (3.3) implies

$$J_s\dot{\omega}_d(t + T) + b_s\omega_d(t + T) = u(t + T - T) = u(t) \tag{3.17}$$

Subtracting (3.17) from (3.16), we obtain

$$J_s(\dot{\omega}_e(t) - \dot{\omega}_d(t + T)) + b_s(\omega_e(t) - \omega_d(t + T)) = -J_sC\dot{e}(t) \tag{3.18}$$

Defining $\tilde{\omega}(t) = \omega_e(t) - \omega_d(t+T)$ and rewriting (3.18) implies

$$J_s\dot{\tilde{\omega}}(t) + b_s\tilde{\omega}(t) = -J_sC\dot{e}(t) \tag{3.19}$$

Since trajectories approach the sliding surface ($\sigma = 0$), observer error and its derivative converge to zero at steady state. Therefore, solution of (3.19) as $t \to \infty$ becomes

$$\lim_{t\to\infty} \tilde{\omega}(t) = 0 \tag{3.20}$$

Since $\tilde{\omega}(t) = \omega_e(t) - \omega_d(t+T)$, it follows that

$$\lim_{t\to\infty} \omega_e(t) = \omega_d(t+T) \tag{3.21}$$

Recall that $\omega_d(t) = \omega(t-T_2)$, and thus $\omega_d(t+T) = \omega(t+T-T_2) = \omega(t+T_1)$. Hence, the final result is

$$\lim_{t\to\infty} \omega_e(t) = \omega_d(t+T) = \omega(t+T_1) \tag{3.22}$$

This shows that the sliding mode observer (SMO) predicts future values of slave's velocity. □

3.1.2 Modified Luenberger Observer 1

In observer based approach, using the sliding mode observer (SMO) provides robustness since it is based on sliding mode control (SMC) which is a well known robust control technique. On the other hand, as it will be explained later in this chapter that the slave system could be linearized in terms of nominal parameters by rejecting nonlinear terms, external disturbances and parametric uncertainties using disturbance observer. Thus, modified Luenberger type observers can be designed alternatively. One of the two Luenberger type observers designed as predictor observers that predicts the future positions of the slave is given by the following equations

$$\dot{p_e}(t) = \omega_e(t) \tag{3.23}$$

$$J_s\dot{\omega_e}(t) + b_s\omega_e(t) = u(t) - L(\omega_d(t) - \hat{\omega}(t)) \tag{3.24}$$

$$\dot{\hat{p}}(t) = \hat{\omega}(t) \tag{3.25}$$

$$\dot{\hat{\omega}}(t) = \dot{\omega}_d(t) + K_{v_o}(\omega_d(t) - \hat{\omega}(t)) + K_{p_o}(p_d(t) - \hat{p}(t)) \tag{3.26}$$

where the observer gain parameters are chosen as $L, K_{v_o}, K_{p_o} > 0$. Note that the first two equations of the observer reminds a Luenberger observer that mimics the dynamics of the slave system. The observer errors and its derivatives can also be defined similar to Eqn. (3.8)-(3.11). Eqn (3.26) can be written in the following form

$$\dot{\omega}_d(t) - \dot{\hat{\omega}}(t) + K_{v_o}(\omega_d(t) - \hat{\omega}(t)) + K_{p_o}(p_d(t) - \hat{p}(t)) = 0 \tag{3.27}$$

and substituting the error expressions, we obtain

$$\ddot{e}(t) + K_{v_o}\dot{e}(t) + K_{p_o}e(t) = 0 \tag{3.28}$$

where $K_{p_o} = \omega^2$ (ω: natural frequency of the observer) and $K_{v_o} = 2\omega = 2\sqrt{K_{p_o}}$ for critically damped error response. Consequently, the error approaches to zero exponentially as $t \to \infty$.

Lemma 2. *The observer defined by the equations in (3.23)-(3.26) predicts the future position (and/or velocity) of the slave system.*

Proof. Subtracting Eqn. (3.24) from Eqn. (3.17) we obtain

$$J_s(\dot{\omega}_d(t+T) - \dot{\omega}_e(t)) = -b_s(\omega_d(t+T) - \omega_e(t)) + u(t) - u(t) + L(\omega_d(t) - \hat{\omega}(t)) \tag{3.29}$$

By the following definition

$$\tilde{\omega} = \omega_d(t+T) - \omega_e(t) \tag{3.30}$$

Eqn. (3.29) can be rewritten as

$$J_s\dot{\tilde{\omega}}(t) = -b_s\tilde{\omega}(t) + L(\omega_d(t) - \hat{\omega}(t)) = -b_s\tilde{\omega}(t) + L\dot{e}(t) \tag{3.31}$$

At steady state, derivative of the observer error ($\dot{e} = \omega_d - \hat{\omega}$) and $\dot{\tilde{\omega}}$ converge to zero, i.e. $\dot{e} \to 0$ and $\dot{\tilde{\omega}} \to 0$. Hence, from Eqn. (3.31) we obtain

$$\tilde{\omega} \to 0 \qquad as \qquad t \to \infty \tag{3.32}$$

which implies

$$\lim_{t\to\infty} \omega_e(t) = \omega_d(t+T) = \omega(t+T_1) \tag{3.33}$$

□

3.1.3 Modified Luenberger Observer 2

The first Luenberger type observer and SMO require angular acceleration information which is calculated by Euler's backward difference method from the angular velocity. Such an approximate derivative may degrade the system performance due to high frequency noises. Although any problem has not been encountered in experiments performed with SMO, an observer that doesn't require acceleration information can be useful. Thus an observer with the following equations is proposed:

$$\dot{p_e}(t) = \omega_e(t) \tag{3.34}$$

$$J_s\dot{\omega_e}(t) + b_s\omega_e(t) = u(t) - L(p_d(t) - \hat{p}(t)) \tag{3.35}$$

$$\dot{\hat{p}}(t) = \hat{\omega}(t) \tag{3.36}$$

$$\dot{\hat{\omega}}(t) = \dot{\omega}_d(t) + K_{p_o}(p_d(t) - \hat{p}(t)) \tag{3.37}$$

Lemma 3. *The observer defined by the equations in (3.34)-(3.37) predicts the future position (and/or velocity) of the slave system.*

Proof. Defining the observer error and its derivative as Eqn. (3.8) and Eqn. (3.9), Eqn. (3.37) can be reorganized as

$$\dot{e}(t) + K_{p_o}e(t) = 0 \tag{3.38}$$

In this observer, the error dynamics is given with a first degree equation whose solution is calculated as

$$e(t) = exp(-K_{p_o}t)e(0) \tag{3.39}$$

where it can be observed that the error converges to zero as $t \to \infty$. By subtracting Eqn. (3.35) from Eqn. (3.17) we obtain

$$J_s\dot{\tilde{\omega}}(t) = -b_s\tilde{\omega}(t) + L(p_d(t) - \hat{p}(t)) \tag{3.40}$$

where the convergence of the position error $(p_d - \hat{p})$ to zero yields

$$\lim_{t\to\infty} \omega_e(t) = \omega_d(t+T) = \omega(t+T_1) \tag{3.41}$$

$\square$

3.1.4 Controller Design

Estimated (or predicted) velocity $\omega_e(t) = \omega(t+T_1)$ and its integral $p_e = p(t+T_1)$ can be used in controller design (see Figure 3.2).

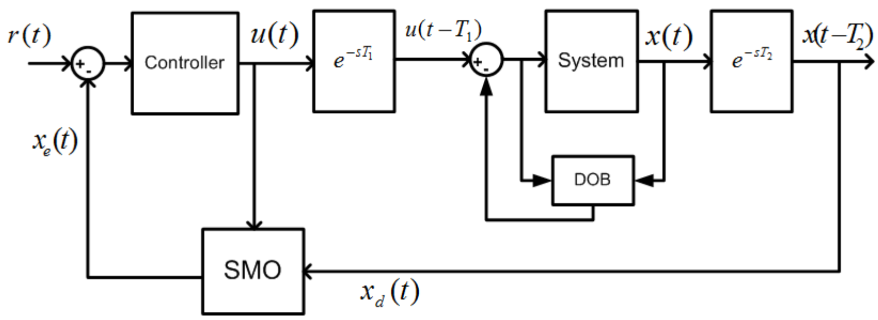

Figure 3.2: SMO Based Bilateral Control System

Control signal $u(t)$ for the slave can be designed as

$$u(t) = f(X_e(t)) = f(p_e(t), \omega_e(t)) \tag{3.42}$$

where $f(.)$ is a linear or nonlinear function. For instance, $f(.)$ could represent a linear control such as PD or a robust nonlinear control such as SMC (sliding mode control). Since the designed control input is delayed by T_1 through the channel, in light of (3.42) slave control input $\tau_s(t)$ can be written as

$$\tau_s(t) = u(t-T_1) = f(p_e(t-T_1), \omega_e(t-T_1))$$

Since $p_e(t) = p_d(t+T)$ the expression becomes as

$$u(t - T_1) = f(p_d(t + T_2), \omega_d(t + T_2)) \tag{3.43}$$

where the control signal finally results in

$$u(t - T_1) = f(p(t), \omega(t)) \tag{3.44}$$

Equation (3.44) shows that the slave control input $\tau_s(t)$ is designed in terms of non-delayed signals, and thus the slave system is automatically stable.

3.2 Disturbance Observers

In order to implement the proposed time delay compensation method on nonlinear teleoperator systems, nonlinear robot dynamics must be linearized. In this work, linearization with disturbance observer method (Fig. 3.3) is proposed for linearization. In addition to the external disturbances, nonlinear terms and parametric uncertainties are also included in the total disturbance. Hence, when the total disturbance is properly compensated, a linear dynamics with nominal parameters is obtained.

Nonlinear dynamics of an n DOF robot manipulator can be written as

$$\tau = D(q)\ddot{q} + C(q, \dot{q})\dot{q} + F_G(q) + B\dot{q} + \tau_d \tag{3.45}$$

where q is the vector of joint angles, $D(q)$ is the $n \times n$ positive-definite inertia matrix, $C(q, \dot{q})$ is the $n \times n$ Coriolis-centripetal matrix, $F_G(q)$ is the $n \times 1$ gravitational force vector, B is the viscous friction (damping) matrix, τ_d is an external disturbance vector and τ is the control input vector.

We first note that inertia and damping matrices can be written as

$$D(q) = D_{nom} + \tilde{D}(q)$$

and

$$B = B_{nom} + \tilde{B}$$

where the nominal inertia and damping matrices are defined as

$$D_{nom} = diag(J_{nom_1}, J_{nom_2}, \ldots, J_{nom_n})$$

and

$$B_{nom} = diag(b_{nom_1}, b_{nom_2}, \ldots, b_{nom_n})$$

Rewriting Eqn. ((3.45)) in terms of nominal inertia and damping matrices imply

$$D_{nom}\ddot{q} + B_{nom}\dot{q} + \tau_{dis} = u \tag{3.46}$$

where u is the control input and τ_{dis} is the total disturbance acting on the system which is defined as

$$\tau_{dis} = \tilde{D}(q)\ddot{q} + C(q, \dot{q})\dot{q} + \tilde{B}\dot{q} + F_G(q) + \tau_d \tag{3.47}$$

where $\tilde{(.)}$ represents the difference between the actual and nominal quantities. In order to estimate the total disturbance at each joint, a disturbance observer [67] is integrated to each joint of the robot (see Fig. 3.3).

In Fig. 3.3, $P_{nom_i}(s)$ denotes the nominal transfer function of the linear system, characterized by the actual transfer function $P_i(s)$, modeling each

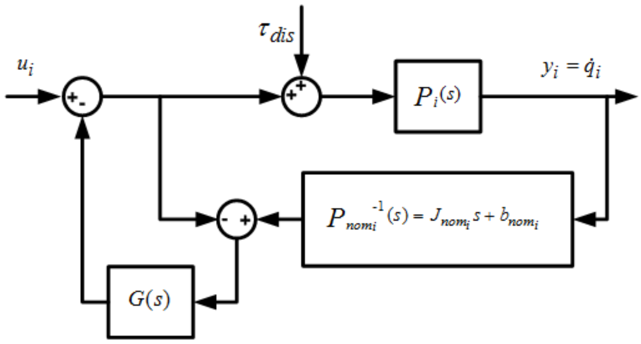

Figure 3.3: Disturbance Observer

joint (i) and $G(s) = \frac{g}{s+g}$ is the transfer function of the low-pass filter used to estimate the total disturbance. By using superposition, the system output can be written [68] as

$$y_i = G_{u_i - y_i}(s)u_i + G_{\tau_{dis} - y_i}(s)\tau_{dis} \tag{3.48}$$

where

$$G_{u_i - y_i}(s) = \frac{P_i(s)P_{nom_i}(s)}{P_{nom_i}(s) + (P_i(s) - P_{nom_i}(s))G(s)} \tag{3.49}$$

and

$$G_{\tau_{dis} - y_i}(s) = \frac{P_i(s)P_{nom_i}(s)(1 - G(s))}{P_{nom_i}(s) + (P_i(s) - P_{nom_i}(s))G(s)} \tag{3.50}$$

If $G(s) \approx 1$, then the transfer functions given in (3.48)-(3.50) are approximated as

$$G_{u_i - y_i}(s) \approx P_{nom_i}(s) = \frac{1}{J_{nom_i}s + b_{nom_i}} \tag{3.51}$$

and

$$G_{\tau_{dis} - y_i}(s) \approx 0 \tag{3.52}$$

Equations (3.51) and (3.52) show that the total disturbance acting on the system is eliminated in the low frequency region characterized by the filter's cut-off frequency and the input/output relationship of the system is linear with nominal parameters. As a result, the nonlinear robot dynamics given in (3.45) will be reduced to the following linear dynamics

$$J_{nom_i}\ddot{q}_i + b_{nom_i}\dot{q}_i = u_i, \quad i = 1, 2, \ldots, n \tag{3.53}$$

Notice that Eqn. ((3.53)) can be used for both slave and master robots described in equations (1) and (2). Thus, the delay compensation method detailed in the previous section can be used for the position control of nonlinear bilateral teleoperator systems.

Chapter IV

4 Force Reflecting Bilateral Teleoperation

Bilateral teleoperation enables a human operator to manipulate a remote teleoperator (slave) and feel the interaction forces between the environment and slave by providing force feedback. In order to provide the human to be kinesthetically coupled with the environment, impedances at each side of the communication channel should be matched ($Z_t = Z_e$). However, due to the inevitable communication delay, identical impedances at both sites (transparency) cannot be achieved. Hence, the well known four channel control structure is modified by the integration of the proposed prediction based delay compensation technique in order to achieve stable and transparent teleoperation.

4.1 Modified Force Based Predictor Observer

In the proposed delay compensation scheme control input is designed at the master side by using the future values of the slave's states and sent to the slave. In free motion, the system works in the structure given in Fig. 2.3. When contact with environment is considered, the slave system does not require any information from master side except the control input. Therefore for the delay compensation technique that combines both SMO and four channel controller structure, the fourth channel is revealed as unnecessary.

Then, the proposed control architecture becomes three channel controller where control torque, environment torque and slave position are transmitted (Fig. 4.1).

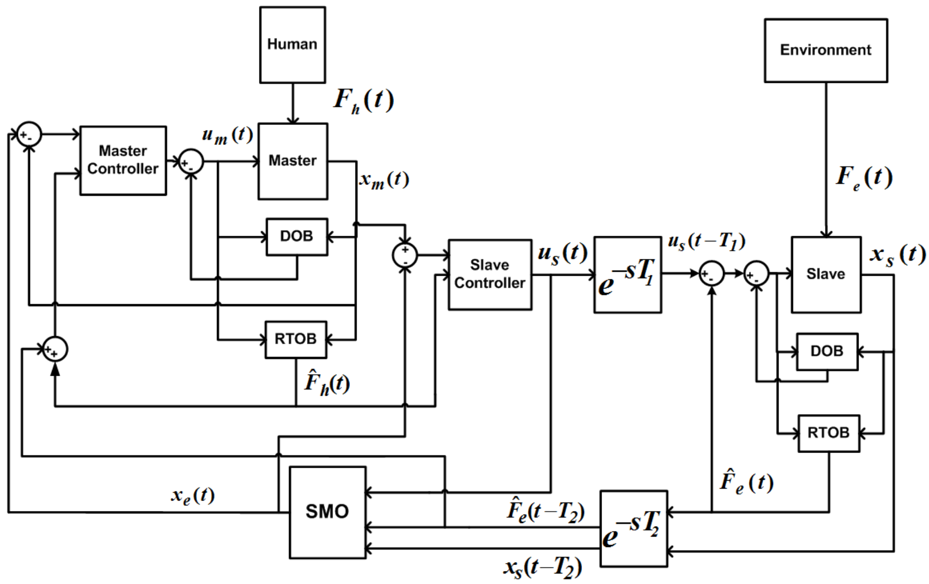

Figure 4.1: Three channel controller and predictor SMO

Acceleration control is performed on both the master and slave robots. In the master side Proportional-Derivative (PD) controller that pushes master's position to slave's estimated position and a force controller that yields the estimated human force to be equal to the estimated environment force with opposite sign are combined. The equation that provide control reference in acceleration dimension for master is given as

$$\ddot{x}_m(t) = K_{p_m}(x_e(t) - x_m(t)) + K_{d_m}(\dot{x}_e(t) - \dot{x}_m(t)) - K_{f_m}(\hat{F}_e(t - T_2) + \hat{F}_h(t)) \tag{4.1}$$

where $\hat{F}_e$ and $\hat{F}_h$ denote the estimated environment and human forces by 'Reaction Torque Observer (RTOB)' respectively.

For the slave, a PD controller is designed at the master side to push the slave's position to master's position and is combined with the estimated human force ($\hat{F}_h(t)$). The estimated environment force ($\hat{F}_e(t)$) is subtracted from this control input at the slave side. The acceleration controller that is designed at the master side is defined as

$$\ddot{x}_s(t) = K_{p_s}(x_m(t) - x_e(t)) + K_{d_s}(\dot{x}_m(t) - \dot{x}_e(t)) - K_{f_s}\hat{F}_h(t) \tag{4.2}$$

Human force acting on the master manipulator, F_h, is estimated at the master side by establishing a RTOB around the master system. Similarly, environment force that is generated when there is a contact with the environment is estimated at the slave side by another RTOB which can be considered as a modified disturbance observer. The idea behind force estimation by RTOB is to extract the disturbance terms other than the external force from the total disturbance estimated by an ordinary disturbance observer (DOB). Parameter uncertainties, system nonlinearities, friction, coupling, gravity can be counted as the disturbances other than the external forces and they should be known exactly to estimate the external forces precisely. This method retrieves us from using additional force sensors. For a nonlinear system given with Eqn. (2.3), total disturbance calculated by a disturbance observer for each joint is given as

$$\tau_{dis} = \tau_{int} + \tau_{ext} + F_i + D_i\dot{q}_i + (J_i - J_{nom_i})\ddot{q}_i + (b_i - b_{nom_i})\dot{q}_i \tag{4.3}$$

where τ_{int} is the interactive torque, including the coupling inertia torque, gravitation etc., τ_{ext} is the reaction torque which is nonzero when the system contacts with the environment, F_i and $D_i\dot{q}_i$ are the Coulomb and viscous friction respectively, $(J_i - J_{nom_i})\ddot{q}_i$ is the self-inertia variation torque and lastly

$(b_i - b_{nom_i})\dot{q}_i$ is the torque pulsation due to the flux distribution variation of the motor. As explained in the previous section, by extracting these forces from the nonlinear system dynamics, a linear system with nominal parameters is obtained (Eqn 3.53). Since the total disturbance is calculated by the disturbance observer, the external torque equation is given as

$$\tau_{ext} = \tau_{dis} - \tau_{int} - F_i - D_i\dot{q}_i - (J_i - J_{nom_i})\ddot{q}_i - (b_i - b_{nom_i})\dot{q}_i \tag{4.4}$$

When the manipulator dynamics are being made nominal with disturbance observers, the external forces are also eliminated from the system and therefore the system behaves as if no forces are acting externally. Master and slave systems are subject to external forces via designed controllers.

The environment force estimated at the slave side is sent to the master side through the communication channel and subject to constant or time-variable delay. SMO is modified to compensate the effects of the delay when the system is in contact with the environment. The modified SMO equations are defined as

$$\dot{\hat{p}}(t) = \hat{\omega}(t) \tag{4.5}$$

$$J_s\dot{\hat{\omega}}(t) + b_s\omega_e(t) = u_s(t) - \hat{F}_e(t - T_2) + u_o(t) \tag{4.6}$$

$$J_s\dot{\omega}_e(t) = J_s\dot{\omega}_d(t) - u_{oeq}(t) \tag{4.7}$$

$$\dot{p}_e(t) = \omega_e(t) \tag{4.8}$$

Observer error and its derivatives are defined as in Eqn. (3.8), Eqn. (3.9) and Eqn. (3.11). Substituting $\dot{\hat{\omega}}(t)$ from Eqn (4.6) into the second derivative yields

$$\ddot{e}(t) = \dot{\omega}_d(t) + \frac{1}{J_s}(b_s(t)\omega_e - u_s(t) - u_o(t) + \hat{F}_e(t - T_2)) \tag{4.9}$$

Since the observer input will be designed in SMC framework, a sliding surface is defined in terms of observer error as in Eqn. (3.12). Substituting error and its derivative into Eqn. 3.12, $\dot{\sigma}$ is obtained as

$$\dot{\sigma} = \dot{\omega}_d(t) + \frac{1}{J_s}(b_s(t)\omega_e - u_s(t) - u_o(t) + \hat{F}_e(t - T_2)) + C\dot{e}(t) \tag{4.10}$$

By setting $\dot{\sigma}$ to zero, we get the equivalent control as

$$u_{oeq}(t) = J_s\dot{\omega}_d(t) + b_s\omega_e(t) - u_s(t) + \hat{F}_e(t - T_2)) + J_sC\dot{e}(t) \tag{4.11}$$

Since the observer input is the sum of the equivalent control $u_{oeq}(t)$ and a discontinuous term ($Ksgn(\sigma)$), we have

$$u_o(t) = u_{oeq}(t) - Ksgn(\sigma) \tag{4.12}$$

which can bring the system onto the sliding surface from arbitrary initial conditions in state-space. Substituting the equivalent control given by (4.11) into (4.7) implies

$$J_s\dot{\omega}_e(t) = -b_s\omega_e(t) + u_s(t) - \hat{F}_e(t - T_2) - J_sC\dot{e}(t) \tag{4.13}$$

When there is contact with the environment the slave dynamics given with

Eqn. (3.3) becomes

$$\begin{aligned} \dot{p}_d(t) &= \omega_d(t) \\ J_s\dot{\omega}_d(t) + b_s\omega_d(t) &= u_s(t-T) - \hat{F}_e(t-T_2) \end{aligned} \tag{4.14}$$

Replacing t by $t+T$ in the second equation of (4.14) implies

$$J_s\dot{\omega}_d(t+T) + b_s\omega_d(t+T) = u_s(t) - \hat{F}_e(t+T_1) \tag{4.15}$$

Subtracting (4.15) from (4.13), we obtain

$$J_s(\dot{\omega}_e(t) - \dot{\omega}_d(t+T)) + b_s(\omega_e(t) - \omega_d(t+T)) = -J_sC\dot{e}(t) + \hat{F}_e(t+T_1) - \hat{F}_e(t-T_2) \tag{4.16}$$

Defining $\tilde{\omega}(t) = \omega_e(t) - \omega_d(t+T)$ and rewriting (4.16) implies

$$J_s\dot{\tilde{\omega}}(t) + b_s\tilde{\omega}(t) = -J_sC\dot{e}(t) + (\hat{F}_e(t+T_1) - \hat{F}_e(t-T_2)) \tag{4.17}$$

At steady state, both observer error (e) and its derivative converge to zero. Since, $\tilde{\omega}$ will converge to a constant value at steady state its derivative will be zero, i.e. $\dot{\tilde{\omega}} = 0$. Note also that since $\lim_{t\to\infty} \hat{F}_e(t+T_1) = \lim_{t\to\infty} \hat{F}_e(t-T_2)$, it follows that

$$\tilde{\omega} \to 0 \qquad as \qquad t \to \infty \tag{4.18}$$

which in turn implies

$$\lim_{t\to\infty} \omega_e(t) = \omega_d(t+T) = \omega(t+T-T_2) = \omega(t+T_1) \tag{4.19}$$

Chapter V

5 Simulations and Experiments

In order to test the success of the proposed method in delay compensation and position tracking performance, simulations and experiments are performed. The simulation and experiment results of predictor based delay compensation method is presented for both free and contact motion of various plants. Simulations are carried out with 2 DOF Scara and pantograph robots which have nonlinear dynamics. For experimental tests, as master and slave systems, a pair of 1 DOF linear manipulators and 2 DOF nonlinear pantograph manipulators are designed and manufactured. In this section, the model and dynamics of the manipulators will be presented together with the simulation and experimental results.

5.1 Simulations for Free Motion

In this subsection, simulations are repeated for two different nonlinear bilateral teleoperation systems where pantograph and scara robots are used as master and slave manipulators. The dynamics of this robots and simulation results for free motion will be presented in this subsection.

5.1.1 Simulations with Scara Robots

In the first simulations, the master and slave manipulators are modeled as a pair of 2 DOF scara robot [70] (see Fig. 5.1). Their corresponding nonlinear dynamics can be written as in (2.3) and (2.4) without subindices:

$$D(q)\ddot{q} + C(q,\dot{q})\dot{q} + F_G(q) + B\dot{q} = \tau$$

In this equation joint angular positions, angular velocities and accelerations are given as $q = [q_1, q_2]^T$, $\dot{q} = [\dot{q}_1, \dot{q}_2]^T$ and $\ddot{q} = [\ddot{q}_1, \ddot{q}_2]^T$, respectively.

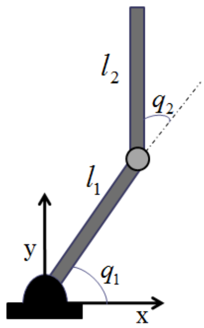

Figure 5.1: Scara Robot

The inertia matrix $D(q)$ is given by

$$D(q) = \begin{bmatrix} m_1 l_{c1}^2 + I_1 + \xi + \gamma & \gamma \\ \gamma & m_2 l_{c2}^2 + I_2 \end{bmatrix}$$

where $\gamma = m_2(l_{c2}^2 + l_1 l_{c2} \cos q_2) + I_2$ and $\xi = m_2(l_1^2 + l_1 l_{c2} \cos q_2)$. In this equation I_i is the link inertia , m_i is the link mass, l_i is the link length and l_{ci} is the joint to the center of mass distance where subindices $i = 1, 2$ denote corresponding link (see Table 5.1). Coriolis and centripetal forces are modeled as the matrix $C(q, \dot{q})$ which is

$$C(q, \dot{q}) = \begin{bmatrix} -\zeta \dot{q}_2 & -\zeta(\dot{q}_1 + \dot{q}_2) \\ \zeta \dot{q}_1 & 0 \end{bmatrix}$$

where $\zeta = m_2 l_1 l_{c2} \sin q_2$. Viscous friction is modeled as $B = diag(b_1, b_2)$ (see Table 5.1) and gravitational forces are taken as $F_G(q) = 0$ since robots are planar.

Table 5.1: Scara Parameters

	Link 1	Link 2
Link Length (l_i)	0.38 m	0.75 m
Distance to Center of Mass (l_{ci})	0.225 m	0.09 m
Mass (m_i)	17.8 kg	3.25 kg
Inertia (I_i)	0.54 kgm^2	0.04 kgm^2
Viscous Friction Coeff. (b_i)	3 Nms/rad	0.6 Nms/rad

Nonlinearities of the system are rejected by disturbance observers and the dynamics of the scara is made nominal. The nonlinear dynamics of the robot is reduced to the linear equation given in Eqn. (3.53) which can be used for both slave and master robots and the proposed delay compensation method can be applied on these linearized dynamics.

System performance is tested under constant and variable delay conditions in the communication channel. The simulations have been carried out using Matlab/Simulink. Constant or variable delay is introduced to the system from the Time Variable Delay block of Simulink library. First, the simulations are performed for the existence of 0.5 sec. constant delay in the communication channel. The human force is simulated as various kinds of reference signals. Simulations with smoothed step, sinusoidal and trapezoidal references under constant delay are presented in this subsection.

The joint positions and end effector positions of the scara robots in cartesian space for a quadratic smoothed step reference are given in Fig. 5.2 and Fig. 5.3 respectively. The control parameters of the PD controller (K_p, K_d) are selected to be $K_p = 50$, $K_d = 1$ for the first joint and $K_p = 30$, $K_d = 2$ for the second joint. The cut-off frequencies of the low-pass filters used in the disturbance observers are set to $g_1 = 50$ rad/sec and $g_2 = 50$ rad/sec. In Fig. 5.2, the 0.5 sec. delay can be noticed in the beginning of the motion. Slave system follows the master system with a 0.5 sec. delay but as the master trajectory settles in a constant position, slave position also converges to master position. Fig. 5.3 shows the end-effector position of master and slave manipulators in cartesian space and as the slave follows the master position successfully, master and slave positions are coincident.

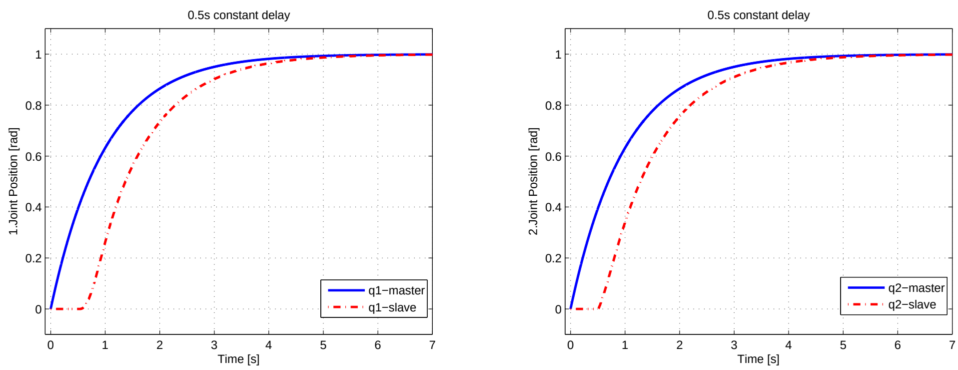

Figure 5.2: Joint positions tracking a smoothed step reference

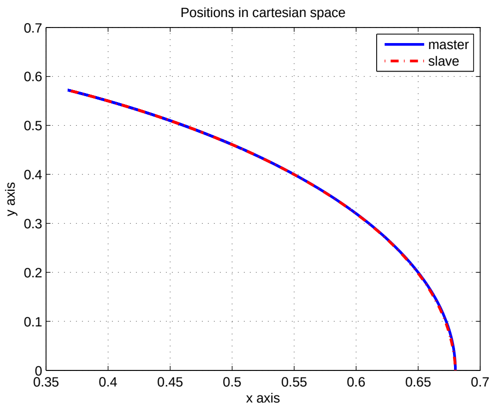

Figure 5.3: Trajectory of the end-effector in $x - y$ plane

As a continuous and periodic trajectory a sinusoidal reference is applied to the system. The phase shift is again observed in the beginning of the motion and did not change during the periodic motion. This behavior is evident from the joint motions (Fig. 5.4) and position tracking is clear from the end-effector positions (Fig. 5.5).

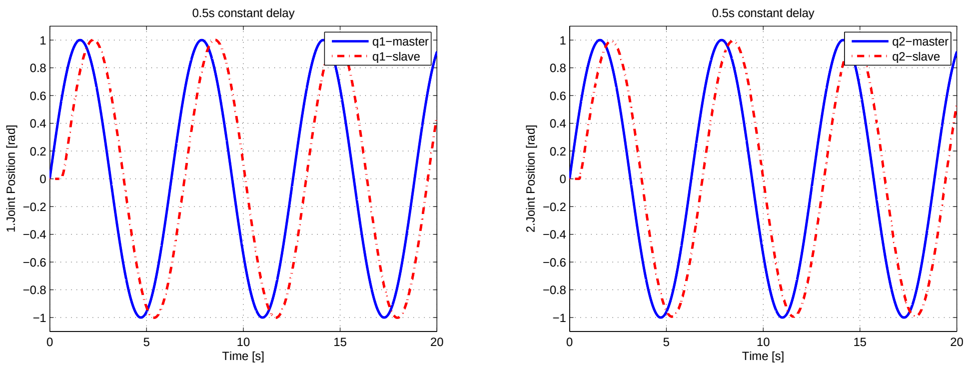

Figure 5.4: Joint positions tracking a sinusoidal trajectory

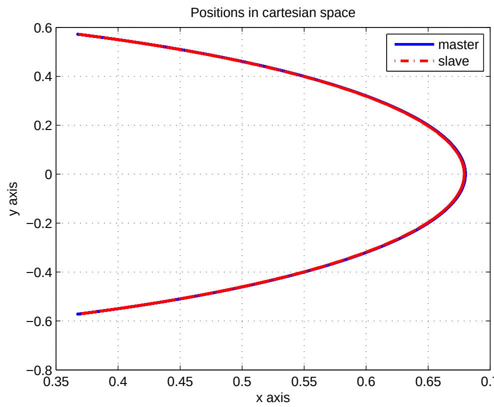

Figure 5.5: Trajectory of the end-effector in $x - y$ plane

As a different trajectory, a trapezoidal position reference is applied to the master scara model. It is observed that the slave cannot follow the master precisely when the trajectory comes to corner points where the direction is suddenly changed. The results are given in Fig. 5.6 and Fig. 5.7.

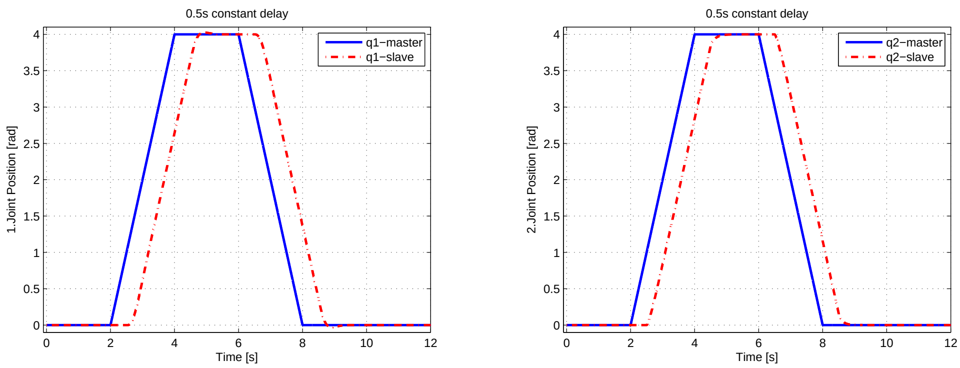

Figure 5.6: Joint positions tracking a trapezoidal trajectory

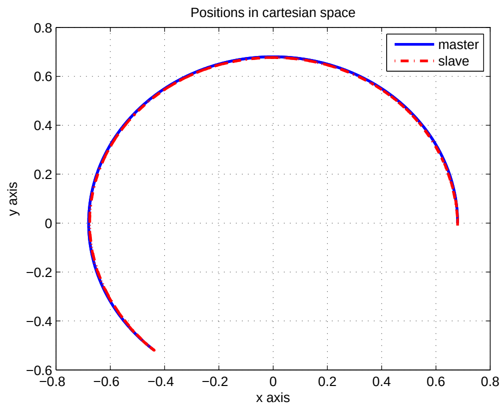

Figure 5.7: Trajectory of the end-effector in $x - y$ plane

Simulation results show that the proposed linearization and delay compensation method works successfully on a 2 DOF nonlinear scara robot when the system is incurred to constant delay.

Results showing that the system behavior does not change with fluctuations of delay will be presented next. In this part, variable delay whose value changes randomly with a mean of 0.5 sec and standard deviation of 0.05 sec. is applied to the system using the Time Variable Delay block. In the first simulations it is considered that the master system generates a smoothed step reference and the performance of the slave manipulator in tracking this reference under variable communication delay is tested. From the joint positions given in Fig. 5.8, a phase shift whose value changes dependending on the delay value is observed. Since the delay changes with a small variability, a significant difference with the constant delay results is not observed. In Fig. 5.8 and Fig. 5.9 the tracking performance is identical with the performance under constant delay.

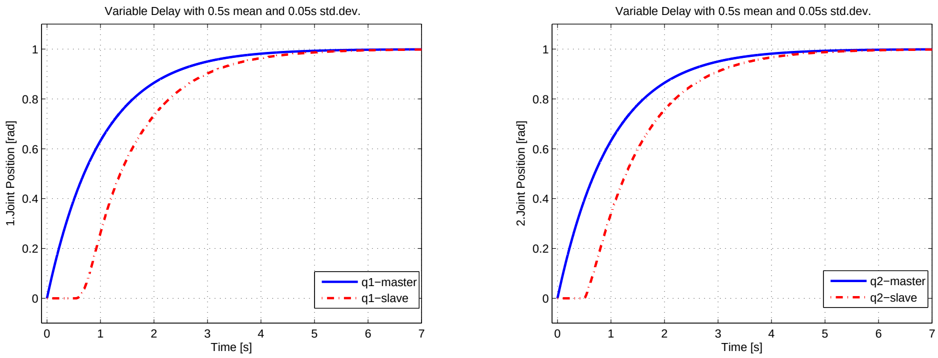

Figure 5.8: Joint positions tracking a smoothed step reference

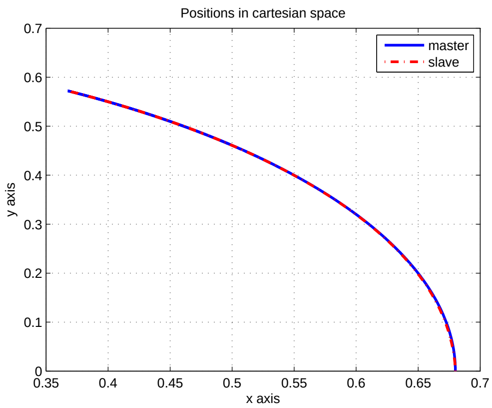

Figure 5.9: Trajectory of the end-effector in $x - y$ plane

As destabilization or performance degradation is not caused by delay variations, the position tracking performance of the system is tested for a periodic reference. As seen in Fig. 5.10 and Fig. 5.11, slave system follows the master with a phase shift whose value changes randomly between 0.276 and 0.724.

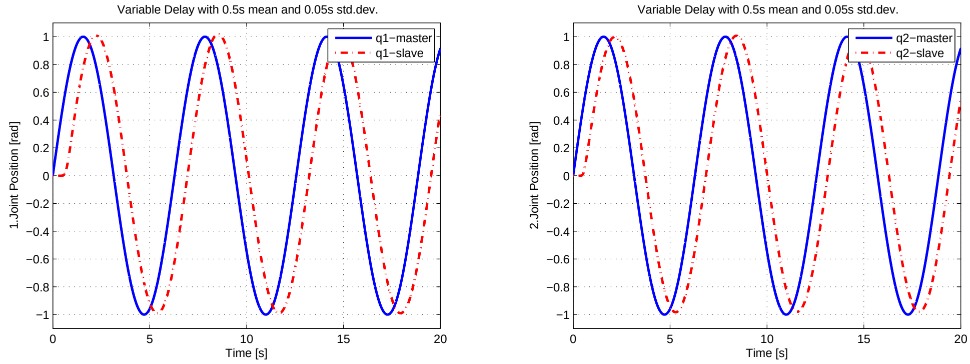

Figure 5.10: Joint positions tracking a sinusoidal trajectory

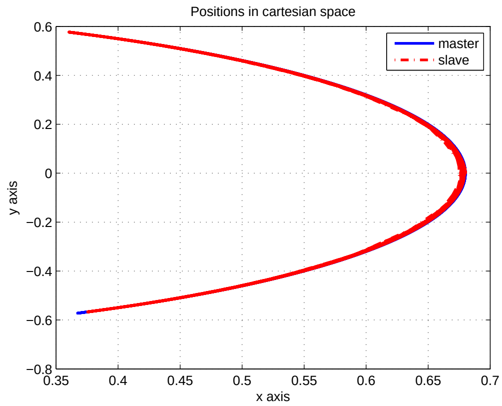

Figure 5.11: Trajectory of the end-effector in $x - y$ plane

When trapezoidal references are applied to the joints of the scara robot, the results given in Eqn. (5.12) and Eqn. (5.13) are obtained and it is observed that they are not different from the constant delay results as expected.

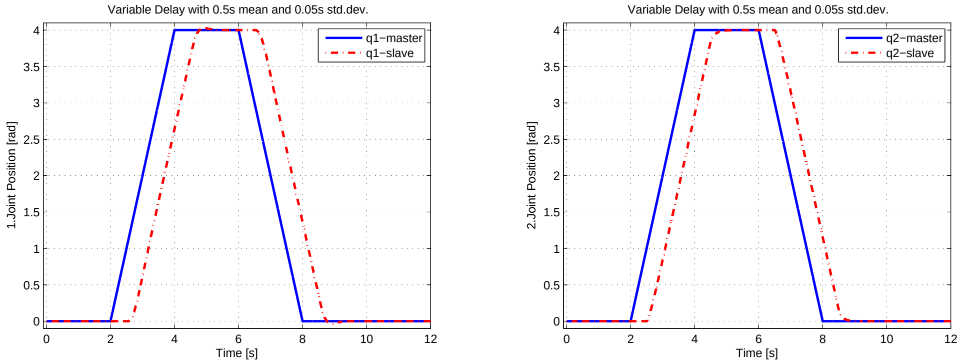

Figure 5.12: Joint positions tracking a trapezoidal trajectory

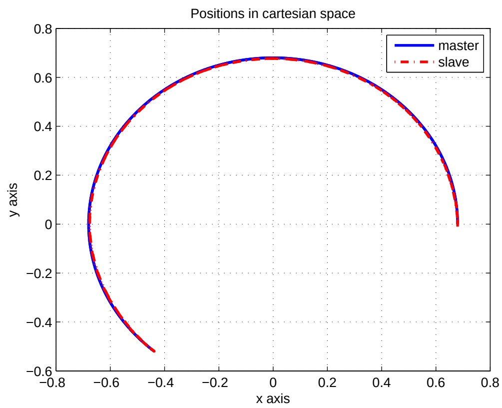

Figure 5.13: Trajectory of the end-effector in $x - y$ plane

The proposed delay compensation method is tested on a 2 DOF scara manipulator under constant or variable communication delay and it is observed that the system stability is achieved for both of the delays and the position tracking performance is quite satisfactory.

5.1.2 Simulations with Pantograph Robots

The method is tested on a different bilateral teleoperation system which is composed of two pantograph robots. Pantograph has a more complex dynamics with its 5−link closed chain mechanism. Like scara, it is also a 2 DOF manipulator but it has two actuated and two passive joints (Fig. 5.14). Since it has a closed-chain structure, derivation of dynamic equations of motion requires highly complex dynamics and kinematics analyses. By utilizing these analyses, dynamic equations of motion of pantograph can be expressed by two actuated joint variables. As explained in [69], equation of motion of pantograph, that lies in horizontal plane, can be written as :

$$\tau_{12} = D(q_i)\ddot{q}_{12} + C(q_i)\dot{q}_{12} \tag{5.1}$$

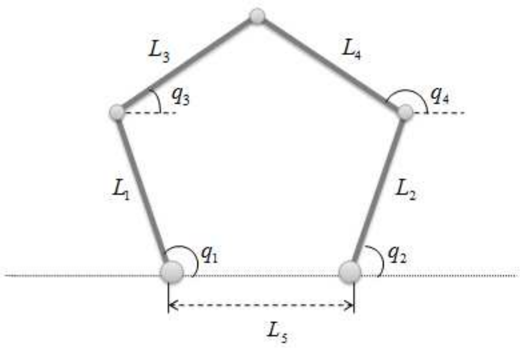

Figure 5.14: Five-link parallel manipulator pantograph

Since gravity is perpendicular to motion plane, gravitational forces do not have effect on equation of motion. In equation (5.1), q_i and $\dot{q}_i$ are the joint angles and angular velocities where $i = 1, 2, 3, 4$, $D(q_i)$ is 2×2 inertia matrix and $C(q_i, \dot{q}_i)$ is 2×2 matrix that contains Coriolis and centripetal forces. The angular acceleration, velocity and input torques of the pantograph are represented by 2×1 vectors $\ddot{q}_{12}$ and $\dot{q}_{12}$ and τ_{12}, respectively.

$D(q_i)$ can be written in terms of moment of inertia, mass, length and positions of the pantograph links as:

$$\begin{aligned} D(q_i) = I_{12} + (A_{34}^{-1}A_{12})^T I_{34} A_{34}^{-1} A_{12} + A_s^T M_{12} A_s + \\ (A_{s34}A_{34}^{-1}A_{12} + A_s)^T M_{34} (A_{s34}A_{34}^{-1}A_{12} + A_s) \\ + A_c^T M_{12} A_c + (A_{c34}A_{34}^{-1}A_{12} + A_c)^T M_{34} (A_{c34}A_{34}^{-1}A_{12} + A_c) \end{aligned} \tag{5.2}$$

where link masses M_i and moment of inertias I_i can be written in the form of 2×2 diagonal matrices as:

$$\begin{aligned} M_{12} = \begin{bmatrix} M_1 & 0 \\ 0 & M_2 \end{bmatrix} \quad M_{34} = \begin{bmatrix} M_3 & 0 \\ 0 & M_4 \end{bmatrix} \\ I_{12} = \begin{bmatrix} I_1 & 0 \\ 0 & I_2 \end{bmatrix} \qquad I_{34} = \begin{bmatrix} I_3 & 0 \\ 0 & I_4 \end{bmatrix} \end{aligned} \tag{5.3}$$

Matrices that are used in calculation of $D(q_i)$ given with Eqn. (5.2), are defined as:

$$\begin{aligned} A_{12} = \begin{bmatrix} L_1 s_1 & -L_2 s_2 \\ L_1 c_1 & -L_2 c_2 \end{bmatrix} \quad A_{34} = \begin{bmatrix} -L_3 s_3 & L_4 s_4 \\ -L_3 c_3 & L_4 c_4 \end{bmatrix} \quad A_s = \begin{bmatrix} L_{c_1} s_1 & 0 \\ 0 & L_{c_2} s_2 \end{bmatrix} \\ A_c = \begin{bmatrix} L_{c_1} c_1 & 0 \\ 0 & L_{c_2} c_2 \end{bmatrix} \quad A_{s34} = \begin{bmatrix} L_{c_3} s_3 & 0 \\ 0 & L_{c_4} s_4 \end{bmatrix} \quad A_{c34} = \begin{bmatrix} L_{c_3} c_3 & 0 \\ 0 & L_{c_4} c_4 \end{bmatrix} \end{aligned} \tag{5.4}$$

where s_i and c_i indicate $sin(q_i)$ and $cos(q_i)$ of the corresponding link, L_{c_i} indicate the distance from center of the links to the joints they belong to and

L_i indicate the link lengths.

The Coriolis-centripetal matrix $C(q_i, \dot{q}_i)$ can be written as the product of derivatives of the elements of matrix $D_(q_i)$ and angular velocities of the pantograph's active links:

$$C(q_i, \dot{q}_i) = \frac{1}{2} \begin{bmatrix} \dot{Q}_{12}^T \begin{bmatrix} \frac{\partial d_{11}}{\partial q_1} \\ 2\frac{\partial d_{11}}{\partial q_1} - \frac{\partial d_{12}}{\partial q_1} \end{bmatrix} & \dot{Q}_{12}^T \begin{bmatrix} \frac{\partial d_{12}}{\partial q_1} \\ 2\frac{\partial d_{12}}{\partial q_1} - \frac{\partial d_{22}}{\partial q_1} \end{bmatrix} \\ \dot{Q}_{12}^T \begin{bmatrix} 2\frac{\partial d_{12}}{\partial q_1} - \frac{\partial d_{11}}{\partial q_2} \\ \frac{\partial d_{12}}{\partial q_2} \end{bmatrix} & \dot{Q}_{12}^T \begin{bmatrix} 2\frac{\partial d_{22}}{\partial q_1} - \frac{\partial d_{12}}{\partial q_2} \\ \frac{\partial d_{22}}{\partial q_2} \end{bmatrix} \end{bmatrix} = \dot{D}(q_i) - C_{KQ}(q_i, \dot{q}_i) \tag{5.5}$$

where $\dot{Q}_{12}^T$ is the vector transpose of the angular angles of pantograph links and $\dot{D}(q_i)$ is time derivative of inertia matrix. In order to simplify the representation of Coriolis-centripetal matrix, the terms except $\dot{D}(q_i)$ are represented by $C_{KQ}(q_i, \dot{q}_i$. The derivative of the inertia matrix given in Eqn. (5.2) can be written as

$$\begin{aligned} \dot{D}(q_i) = {} & 2(A_{34}^{-1}A_{12})^T I_{34} A_{34}^{-1}(\dot{A}_{12} - \dot{A}_{34}\dot{A}_{34}^{-1}A_{12}) \\ & + 2A_s^T M_{12}\dot{A}_s + 2(A_{s34}A_{34}^{-1}A_{12} + A_s)^T M_{34}((\dot{A}_{s34} - A_{s34}\dot{A}_{34}A_{34}^{-1})A_{34}^{-1}A_{12} \\ & + A_{s34}A_{34}^{-1}\dot{A}_1 2 + \dot{A}_s) + 2A_c^T M_{12}\dot{A}_c^+ 2(A_{c34}A_{34}^{-1}A_{12} + A_c)^T M_{34} \\ & ((\dot{A}_{c34} - A_{c34}\dot{A}_{34}A_{34}^{-1})A_{34}^{-1}A_{12} + A_{c34}A_{34}^{-1}\dot{A}_1 2 + \dot{A}_c) \end{aligned} \tag{5.6}$$

where $\dot{A}_{12}$,$\dot{A}_{34}$,$\dot{A}_{s34}$,$\dot{A}_{c34}$,$\dot{A}_{s}$,$\dot{A}_{c}$ can be calculated as:

$$\dot{A}_{12} = \begin{bmatrix} L_1 c_1 \dot{q}_1 & -L_2 c_2 \dot{q}_2 \\ -L_1 s_1 \dot{q}_2 & L_2 s_2 \dot{q}_2 \end{bmatrix} \quad \dot{A}_{34} = \begin{bmatrix} -L_3 c_3 \dot{q}_3 & L_4 c_4 \dot{q}_4 \\ -L_3 s_3 \dot{q}_3 & -L_4 s_4 \dot{q}_4 \end{bmatrix}$$

$$\dot{A}_{s} = \begin{bmatrix} L_{c_1} c_1 \dot{q}_1 & 0 \\ 0 & L_{c_2} c_2 \dot{q}_2 \end{bmatrix} \quad \dot{A}_{c} = \begin{bmatrix} -L_{c_1} s_1 \dot{q}_1 & 0 \\ 0 & -L_{c_2} s_2 \dot{q}_2 \end{bmatrix} \tag{5.7}$$

$$\dot{A}_{s34} = \begin{bmatrix} L_{c_3} c_3 \dot{q}_3 & 0 \\ 0 & L_{c_4} c_4 \dot{q}_4 \end{bmatrix} \quad \dot{A}_{c34} = \begin{bmatrix} -L_{c_3} s_3 \dot{q}_3 & 0 \\ 0 & -L_{c_4} s_4 \dot{q}_4 \end{bmatrix}$$

$C_{KQ}(q_i, \dot{q}_i)$ from Eqn. (5.5) can be written by using Eqn. (5.7) as:

$$C_{KQ}(q_i, \dot{q}_i) = (C_{s34} + C_{34} A_{34}^{-1} A_{12}) \tag{5.8}$$

where C_{34} and C_{s34} are defined as

$$C_{s34} = \begin{bmatrix} -2m_3 L_1 L_{c3} s_1 s_2 \dot{\mathrm{1}}_1 & 0 \\ 0 & -2m_4 L_2 L_{c4} s_2 s_4 \dot{q}_2 \end{bmatrix}$$

$$C_{34} = \begin{bmatrix} (L_1 A_3^{-1} 4 s_{c1})^T & \begin{bmatrix} 2m_3 L_1 L_{c3} s_1 s_3 \dot{q}_1 & 0 \\ 0 & -2m_4 L_2 L_{c4} s_2 s_4 \dot{q}_2 \end{bmatrix} \\ (L_1 A_3^{-1} 4 s_{c2})^T & \begin{bmatrix} 2m_3 L_1 L_{c3} s_1 s_3 \dot{q}_1 & 0 \\ 0 & -2m_4 L_2 L_{c4} s_2 s_4 \dot{q}_2 \end{bmatrix} \end{bmatrix} \tag{5.9}$$

where s_{c1} and s_{c2} terms are represented as $s_{ci} = [sin(q_i) \;\; cos(q_i)]^T$

One of the pantograph robots that is used in the experiments is shown in Fig. 5.15

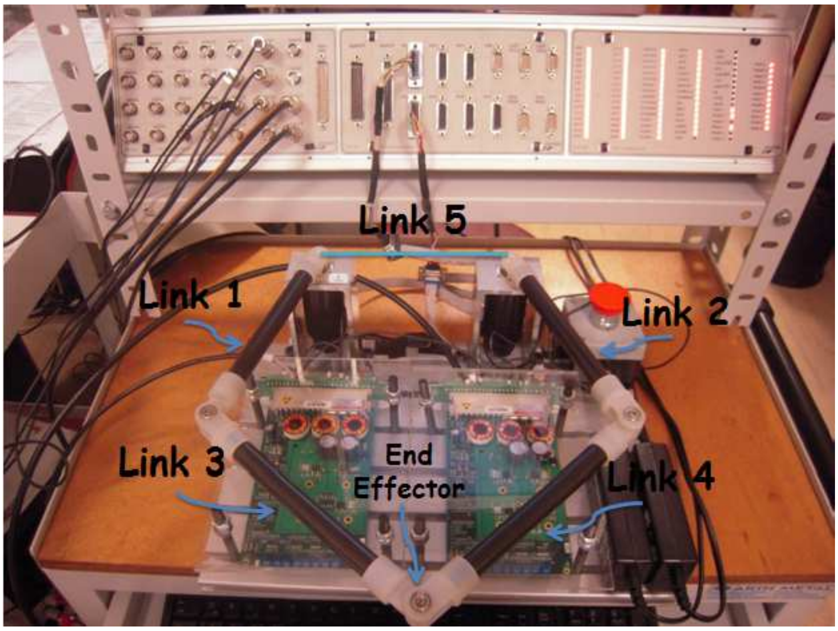

Figure 5.15: Links of pantograph robot

The properties of the pantograph links are given in Table 5.2.

Table 5.2: Technical Properties of Pantograph

	Mass (gr)	Length (mm)	Inertia ($gr.mm^2$)
Link 1	123	200	132,438 $\times$ 10^3
Link 2	123	200	132,438 $\times$ 10^3
Link 3	136	195	141,526 $\times$ 10^3
Link 4	136	195	141,526 $\times$ 10^3
Link 5	-	175	-

Simulations are performed using the 2 DOF and 5 link nonlinear pantograph robots as nonlinear master and slave manipulators which are made nominal by disturbance observer. The control parameters of the system are given in Table 5.3. The cut-off frequency values of the disturbance observers are chosen to be $g_1 = 1500\ rad/sec$ and $g_2 = 1500\ rad/sec$.

Table 5.3: PID Control Parameters for Free Motion Simulations

	K_p	K_d
Joint 1	8	0.4
Joint 2	8	0.4

First it is considered that the communication channel is imposed to constant delay with amount of 0.5 sec. The references are applied to the system as different types of position references. The simulation results with smoothed step references are given in Fig 5.16 and Fig 5.17.

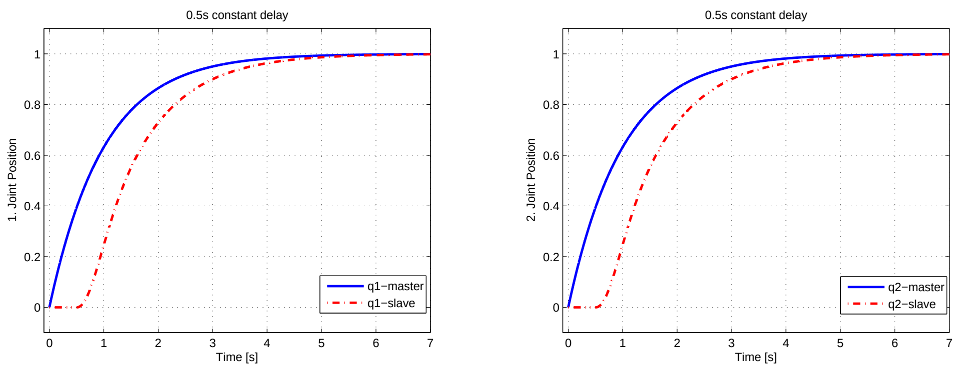

Figure 5.16: Joint positions tracking a smoothed step reference

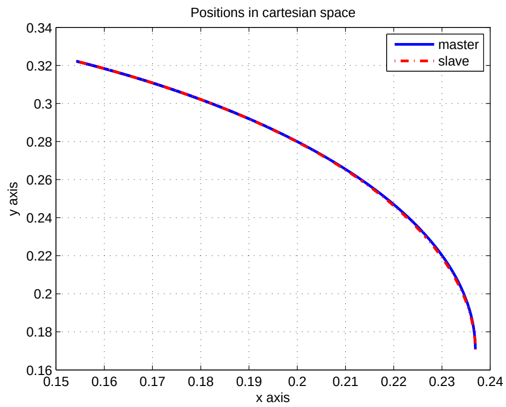

Figure 5.17: Trajectory of the end-effector in $x - y$ plane

It is observed that the slave system successfully tracks the master's position with a constant phase shift of 0.5 sec. which is due to the constant time delay on the communication delay. Simulations are also performed for sinusoidal type of reference and the results are given in Fig. 5.18 and Fig. 5.19. Again 0.5 sec phase shift is significant. It is clearly observed that unstability and performance degradation problems are handled with the proposed method.

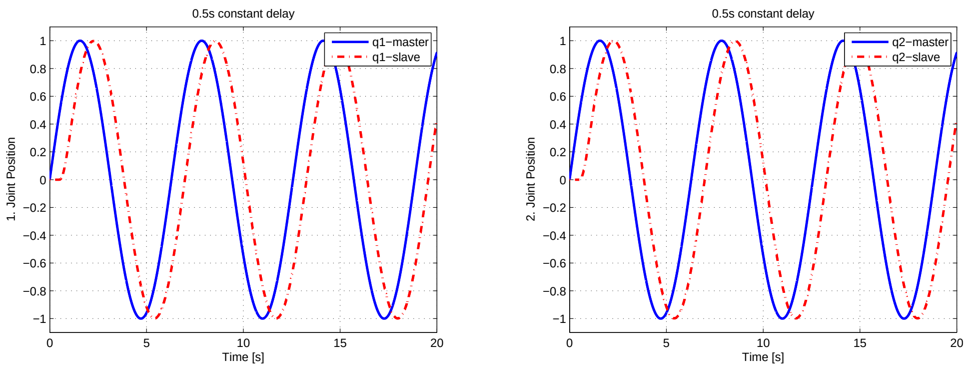

Figure 5.18: Joint positions tracking a sinusoidal reference

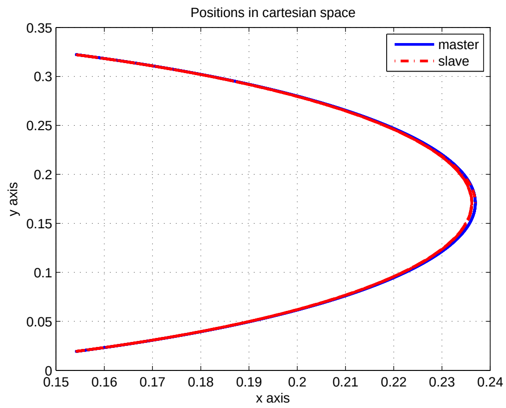

Figure 5.19: Trajectory of the end-effector in $x - y$ plane

In order to observe performance of the method for time variable delay, simulations are carried out on pantograph manipulators. Variable time delay characterized by a normally distributed random variable with a mean of 0.5 sec and standard deviation of 0.05 sec. is applied on the channel and the results of the simulations for smoothed step references are given in Fig 5.20 and Fig 5.21.

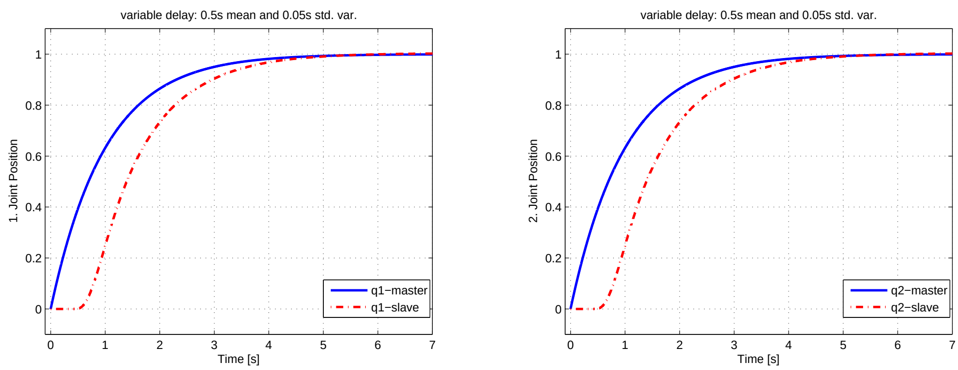

Figure 5.20: Joint positions tracking a smoothed step reference

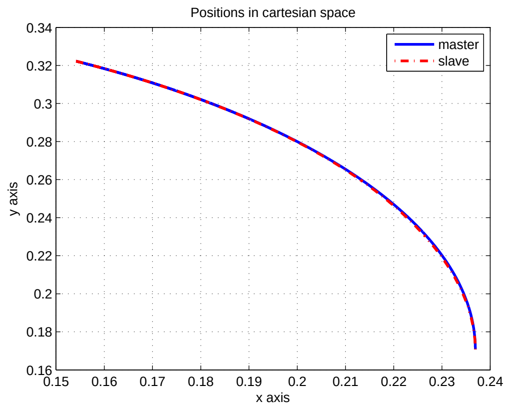

Figure 5.21: Trajectory of the end-effector in $x - y$ plane

Tracking of sinusoidal references by pantograph robots under variable delay results are given in Fig 5.22 and Fig. 5.23.

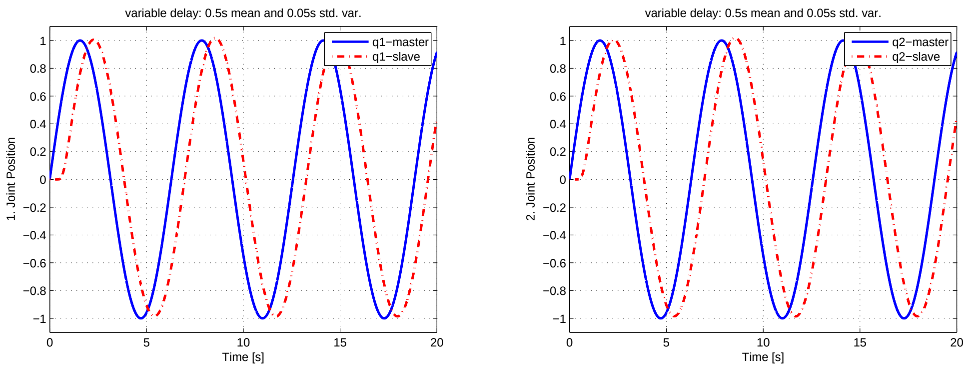

Figure 5.22: Joint positions tracking a sinusoidal reference

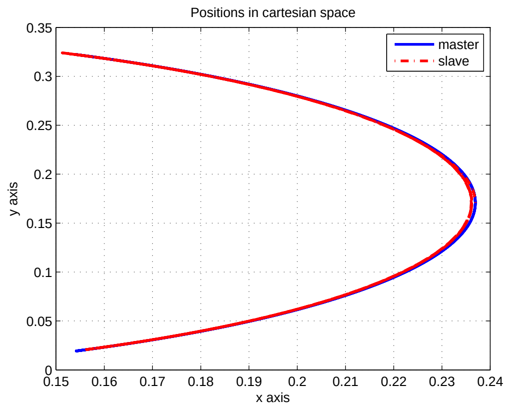

Figure 5.23: Trajectory of the end-effector in $x - y$ plane

Simulation results are similar to the ones obtained with constant delay. The tracking performance is satisfactory and the system does not tend to become unstable.

5.2 Experiments for Free Motion

Two pantograph robots (Fig. 5.24) designed and manufactured in our labs are used in a bilateral control system as master and slave systems.

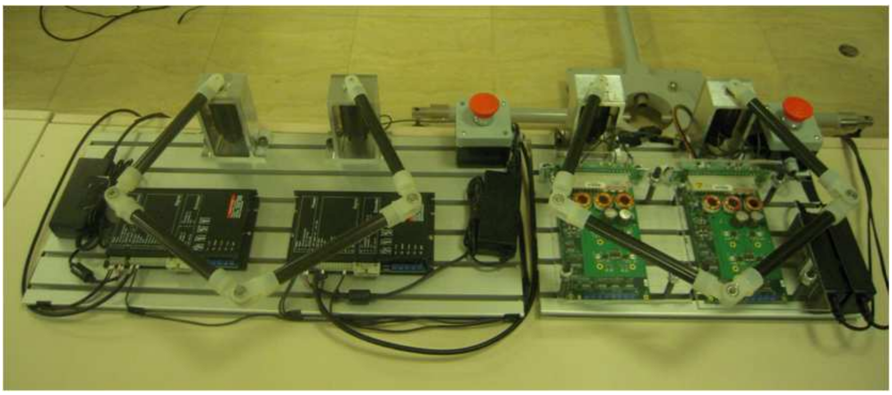

Figure 5.24: Master and slave pantograph robots

Dynamical equations of pantograph robots are linearized using disturbance observer given in the previous section. SMO based time delay compensation method is implemented on these pantograph robots to see the effectiveness of our proposed approach.

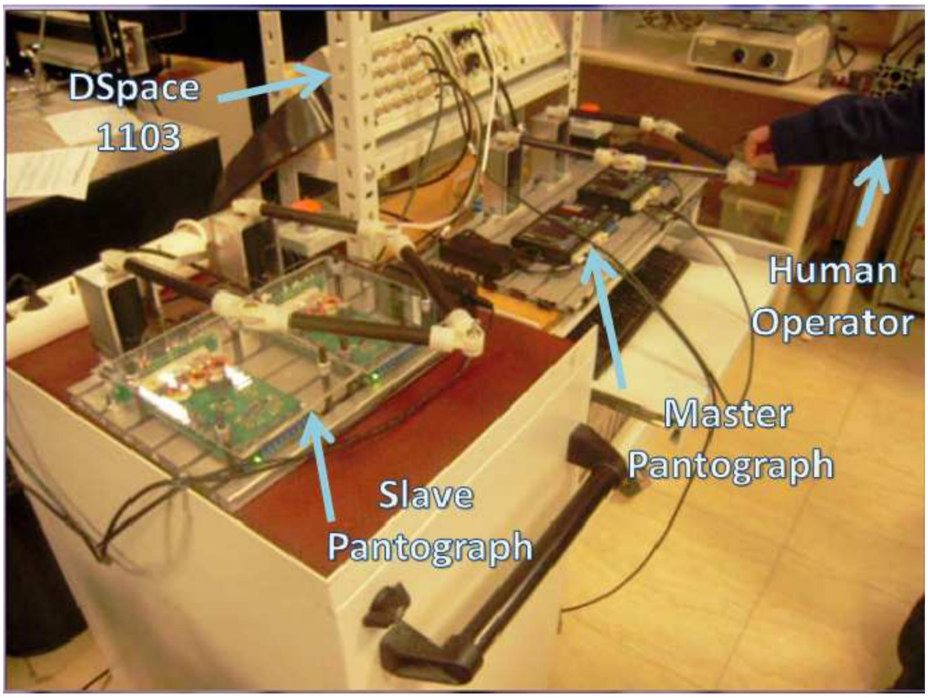

Figure 5.25: Experimental Setup

In the experiments, the end-effector positions of the pantographs in $x - y$ plane and joint angles are examined. The aim is to enable the slave robot to follow master's trajectories generated by human operator. Pantographs are allowed to work in a bilateral teleoperation system by introducing a variable time delay characterized by a normally distributed random variable with a mean of 0.5 sec and standard deviation of 0.025 sec. Time delay is artificially created with Matlab's Time-Variable Delay block. Control algorithms are implemented in real-time using dSpace1103 controller board. The control parameters used in experiments are given in Table 5.4. The cut-off frequency of the low-pass filter, $G(s)$, used in the disturbance observer is set to $g = 1000$ rad/sec.

Table 5.4: PID Control Parameters for Free Motion Experiments

	K_p	K_d
Joint 1	8	0.3
Joint 2	9	0.3

In the first experiment, the human operator holding the end-effector of the master pantograph draws a free-form closed curve. For example, in a remote surgery, an odd-shaped tumor could be represented by a curve like this.

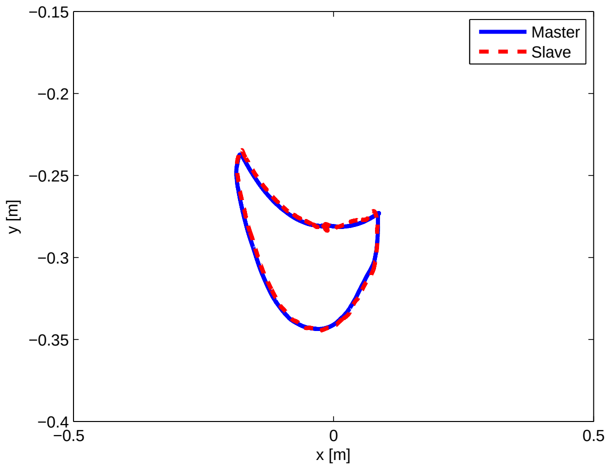

Figure 5.26: Tracking a closed curve

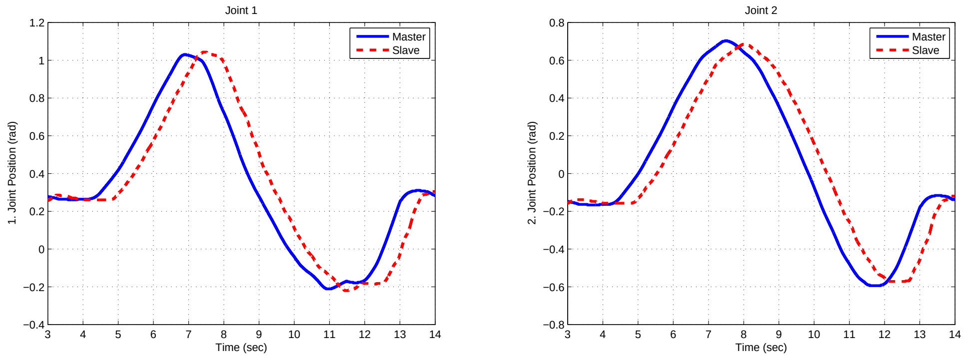

Figure 5.27: Joint positions versus time

As shown in Fig. 5.26, the end-effector of slave pantograph (dashed line) successfully tracks the end-effector of master pantograph (solid line). Angular joint positions of pantographs are depicted in Fig. 5.27. Note that joint angles of pantographs track each other with a delay. This is inevitable since the future values of operator reference can not be known in advance.

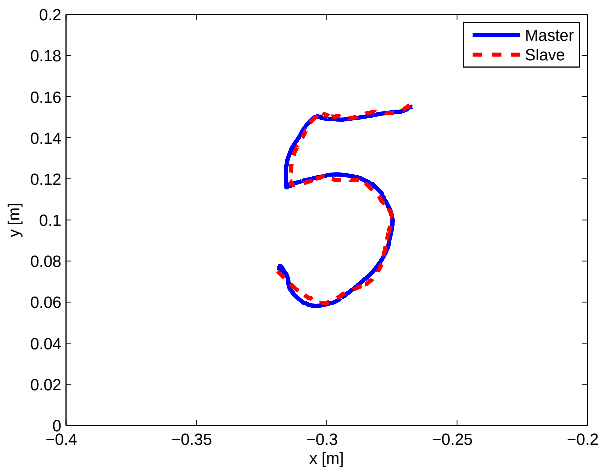

Figure 5.28: Tracking the reference (number 5) drawn by the master

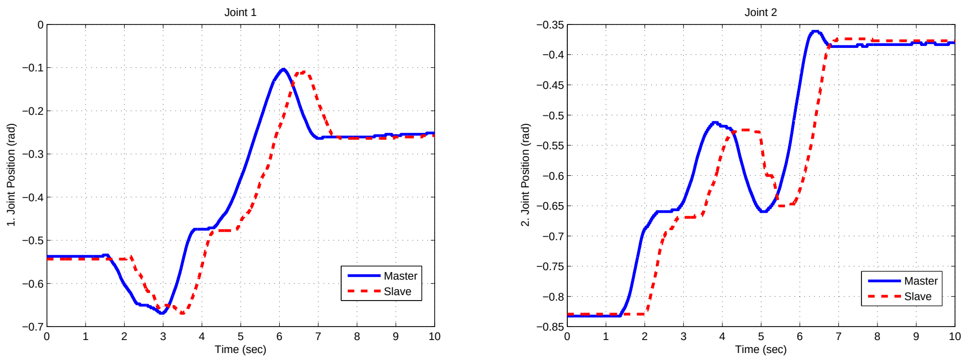

Figure 5.29: Joint positions versus time

In another experiment, number 5 shaped reference (an open curve) is drawn by the operator controlled master pantograph. From Fig. 5.28 and Fig. 5.29 it is clear that slave pantograph successfully tracks this trajectory. Similarly, number 4 shaped reference is also tracked by the slave pantograph quite satisfactorily. Results are shown in Fig 5.30 and 5.31.

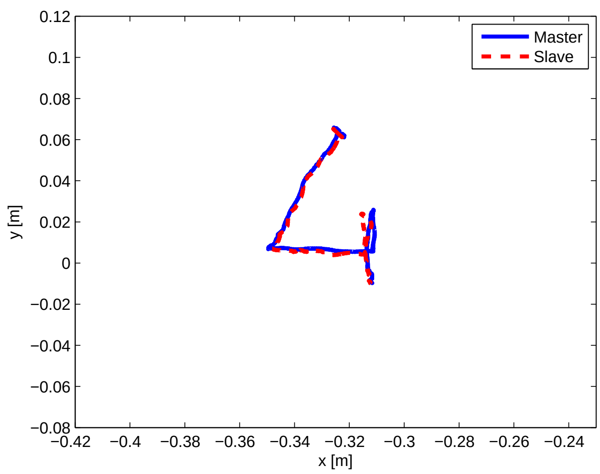

Figure 5.30: Tracking the reference (number 4) drawn by the master

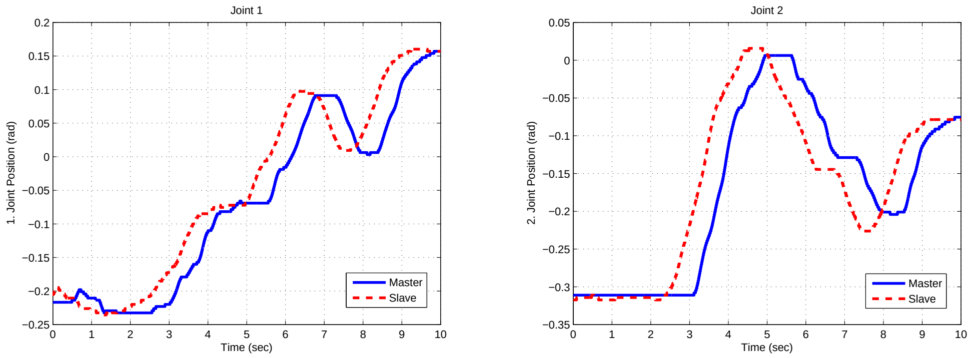

Figure 5.31: Joint positions versus time

Experimental results presented above indicate that the nonlinear dynamics of pantograph robots are successfully linearized and the parameter uncertainties in the system are eliminated by the disturbance observer (DOB) which in turn allows implementation of SMO for delay compensation. In all experiments slave pantograph successfully tracks the trajectory of the master pantograph.

5.3 Simulations for Contact Motion

According to the idea of bilateral teleoperation, when slave system contacts with the environment, the forces applied to the slave should be perceived by the human operator. This goal is achieved by establishing a transparent communication channel between the local and slave manipulators. However, constant or time variable communication delay is inevitable. The system under constant or variable communication delay is stabilized by the proposed method. Moreover, it is possible to feel the environment forces as if human operator directly contacts with the environment. In the previous subsection, it is shown with simulations that, in free motion manipulating a remote system is possible even with a delayed communication. In this subsection the performance of the modified sliding mode observer scheme will be observed on simulation results.

5.3.1 Simulations with Pantograph Robots

In this part, simulations are performed considering the interaction of the slave robot with environment and pantograph robots are used as master and slave manipulators. In order to simulate the contact motion, the environment is modeled as a rigid wall having a rigidity of $k = 1000\ N/m$ and a viscosity of $b = 5\ Ns/m$. Environment force is generated as

$$F_e = k(x_s - x_w) + b\dot{x_s} \tag{5.10}$$

where x_s is the position of the slave and x_w is the position of the wall. The force is generated depending on the end-effector position and it is transformed into joint forces to be applied to the slave joints individually. The parameters used in the simulations are given in Table 5.5.

Table 5.5: Parameters of Simulation

g_{dob}	Cut-off frequency of DOB	1500 rad/sec
g_{rtob}	Cut-off frequency of RTOB	1500 rad/sec
K_p	Position feedback gain	9
K_d	Velocity feedback gain	0.6
K_f	Force feedback gain	1

In the first simulation with constant delay in the channel, the wall is located at $x = 0$ position which means the slave pantograph stops at $x = 0$. The simulation results concerning this scenario is shown in Fig. 5.32 and Fig. 5.33. The second figure of Fig. 5.32 shows the behavior of pantograph's end-effector in x and y coordinates individually. At time $t = 6.16$ sec., the master contacts with the environment at $x = 0$ and as given in the first figure of Fig 5.32 environment force starts to increase. As shown in Fig. 5.33 the trajectory starts at $(x, y) = (0.252, 0.192)$ position and slave stays at $(x, y) = (0, 0.36)$ until the contact force is released. During the contact motion acts on the slave system from the $x-$direction, slave manipulator moves in $y-$direction. When the contact is released at $t = 11$ sec. master and slave manipulators restart free motion from $(x, y) = (0, 0.123)$. Fig. 5.33 shows that the end-effector of the slave cannot exceed the wall position and master pantograph strains to catch slave's position. This means that, the external forces are perceived at the local side. Human force and environment force applied at the contact instants are clearly shown in the first figure of Fig. 5.32. Here it is clear that, trajectories generated by the human operator are tracked with delay by coping with the unstability and performance degradation problem.

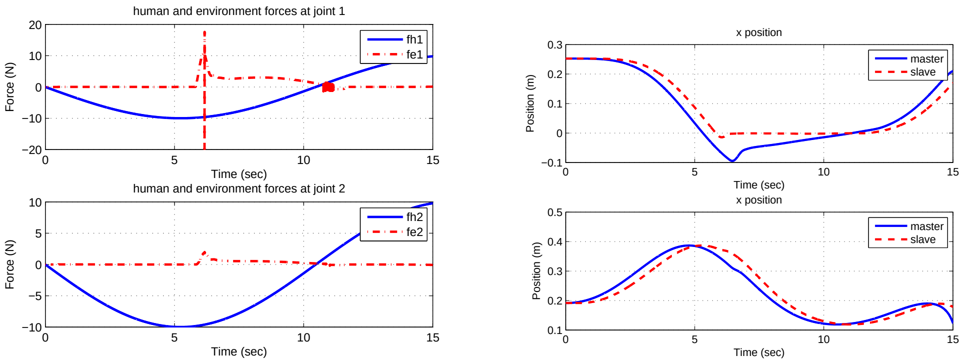

Figure 5.32: External forces and positions in cartesian space

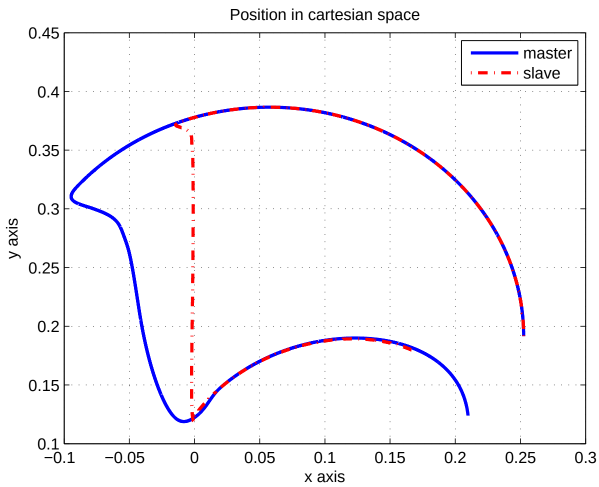

Figure 5.33: Trajectory of the end-effector in $x - y$ plane

As the delay type is interchanged as time variable, Fig. 5.34 and Fig. 5.35 are obtained. The simulation results show that the variable delay is also compensated by the method successfully.

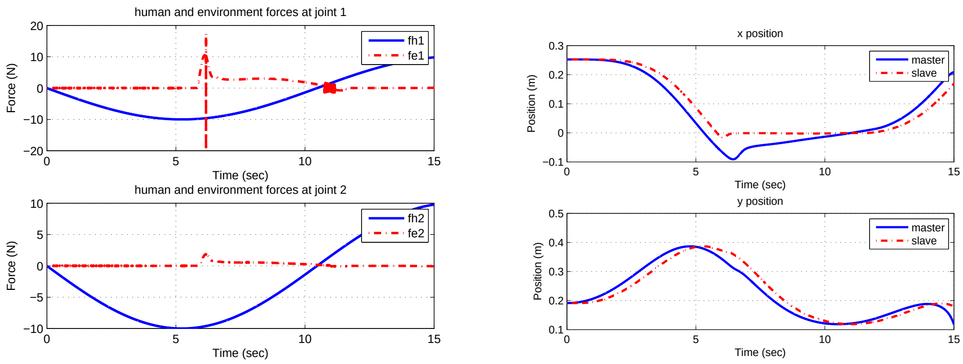

Figure 5.34: External forces and positions in cartesian space

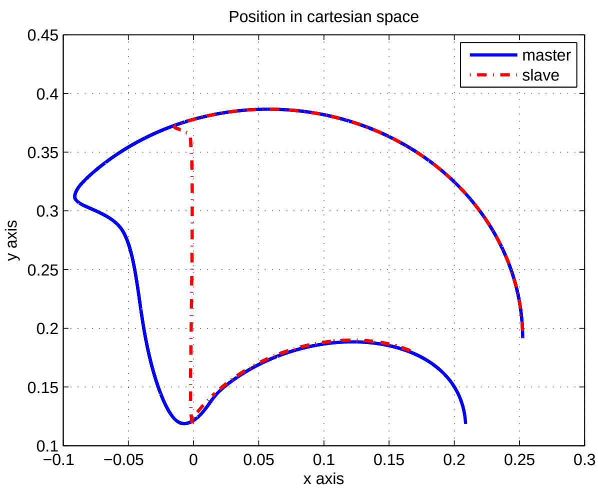

Figure 5.35: Trajectory of the end-effector in $x - y$ plane

5.3.2 Simulations with Scara Robots

As a different plant, scara robots (Fig. 5.1) are used in simulations. In the simulations it is considered that the stiff wall ($k = 1700\ N/m$, $b = 5\ Ns/m$) is located at $y = 0.5$ m. position. The parameters used in the simulations are given in Table 5.6.

Table 5.6: Parameters of Simulation

g_{dob}	Cut-off frequency of DOB	1500 rad/sec
g_{rtob}	Cut-off frequency of RTOB	1500 rad/sec
K_p	Position feedback gain	9
K_d	Velocity feedback gain	0.6
K_f	Force feedback gain	1

As observed from Fig. 5.36, slave robot stops at that position. In the first figure of Fig. 5.36, it is clear that the environment force increases at the moments that contact motion is realized at the assigned wall position.

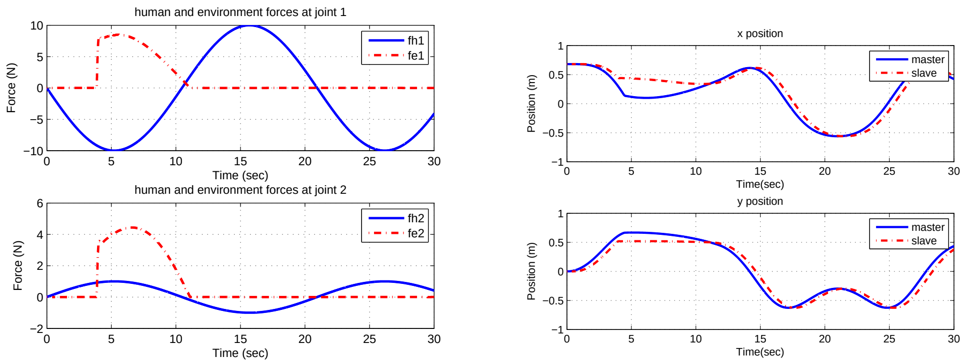

Figure 5.36: External forces and joint positions

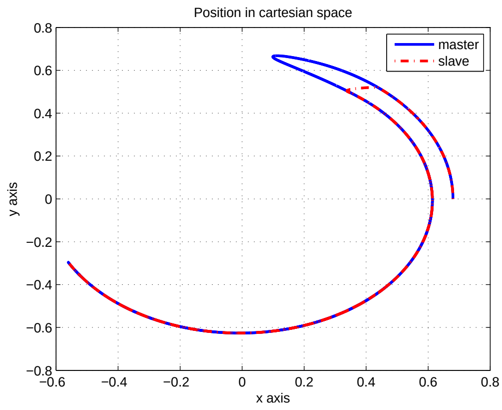

Figure 5.37: Master and slave pantograph robots

Successful results are obtained from the simulations performed with constant delay. Time variable delay is also considered for the scara robot simulations. Similar results with constant delay scenario are obtained as they are given with Fig. 5.38 and Fig. 5.39.

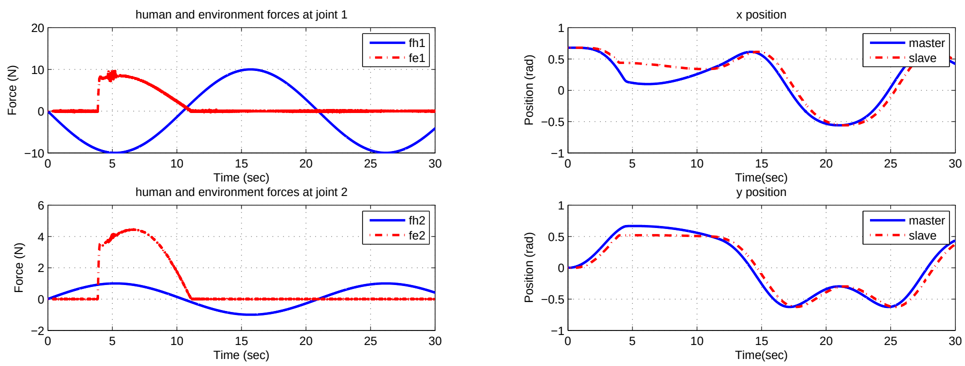

Figure 5.38: External forces and joint positions

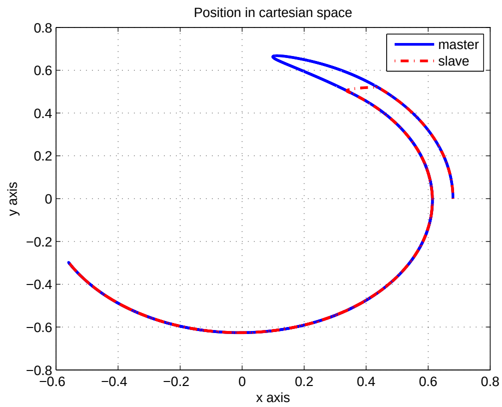

Figure 5.39: Master and slave pantograph robots

5.4 Experiments for Contact Motion

Since the simulation results for contact motion are satisfactory, the method is tested with experiments.

Experiments with 1 link single DOF Robots

Experiments are performed in order to examine performance of the system when contact with environment motion is considered. In experiments, a linear 1 DOF manipulator (Fig. 5.40) is used which means a linearization is not applied on the system. But other disturbances are eliminated with disturbance observers. The environment and human forces are estimated by reaction torque observers. The first figure of Fig. 5.41 shows that at $t = 2.2$ sec the slave manipulator interacts with the environment and cannot move beyond the $y = -0.83$ m. position. During the contact, environment and human forces are increasing in opposite directions as expected. In this experiment the slave system contacts with the environment multiple times.

For instance, at $t = 7.46$ sec., $t = 18.88$ sec. and $t = 29.26$ sec. In the first figure of Fig. 5.41 it is observed that as the human force is increased at the contact motion, the environment force also increased. As observed from Fig. 5.41, due to the communication delay master system perceives the environment force and positions converge each other with delay. When the slave manipulator is released from the wall contact, stable position tracking is achieved with quite satisfactory performance.

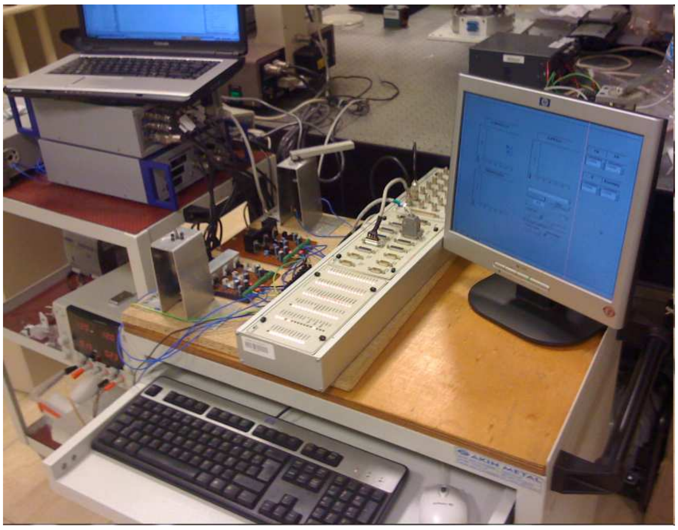

Figure 5.40: Bilateral teleoperation setup with 1 DOF linear manipulators

Experiments are also performed with time variable delay and the results are as shown in Fig 5.42. The slave manipulator contacts with the environment at $t = 6.6$ sec. and as shown in the first figure of Fig. 5.42, environment force starts to increase in that moment until $t = 17.6$ sec. It is observed from the second figure of Fig. 5.42, in this period the slave manipulator does not move from the position of $q = 0.71$ rad. As the contact is released, master and slave positions are converge to each other with a 0.047rad. of steady state error which is negligible.

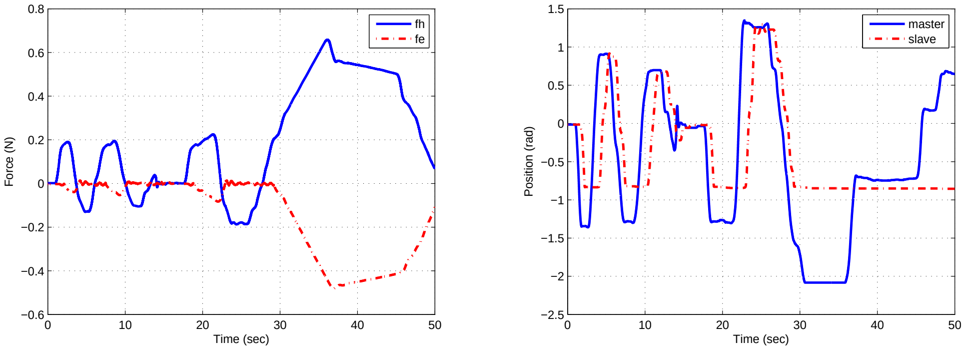

Figure 5.41: Constant delay

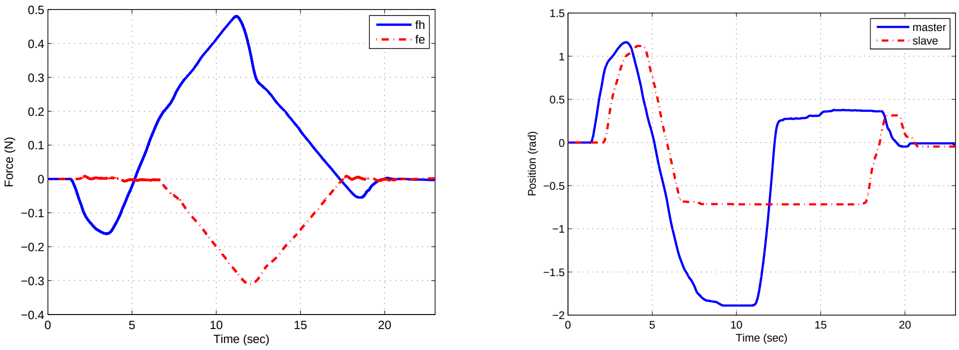

Figure 5.42: Variable delay

From the figures, we can observe that in free motion the master robot follows the slave robot with a phase lag in a stable fashion. When environment contact occurs the estimated human and environment forces become equal in magnitude with opposite signs. However due the phase shift resulting from the communication delay, the master position cannot converge to the slave position immediately. On the other hand, when the contact is released position tracking phase shift is observed.

Experiments with 5 link 2 DOF Pantograph Robots

The proposed three channel controller with SMO is tested on a bilateral teleoperation system composed of two pantograph manipulators Fig.5.25. Experiments are performed under constant and variable delay. In Fig.5.43 the human and environment forces acting on the slave and perceived by the master are shown. As the environment force increases at contact moments, the human force also increases in the opposite direction. Positions of the joints are given in Fig.5.44. At contact moments, the position of the second joint cannot not move and the when the human operator releases the force the master and slave positions converge to each other.

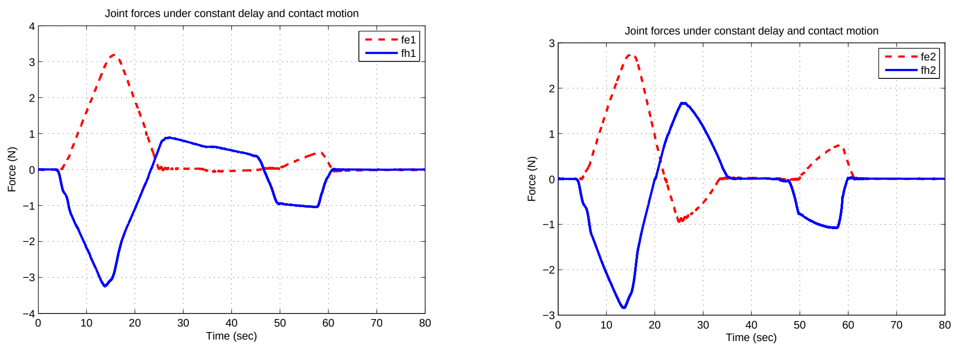

Figure 5.43: Joint Forces

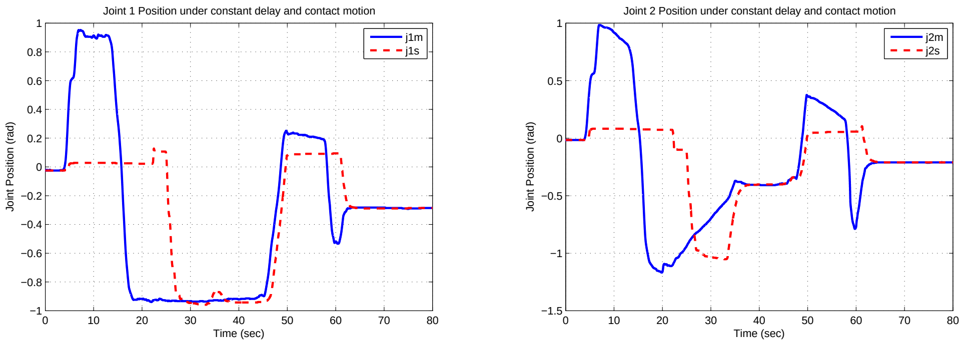

Figure 5.44: Joint Positions

For constant delay, the results are similar to the simulation results. There are some unexpected motions but they can be considered to be caused due to the sudden change of action and reaction forces.

The method is tested also for variable time delay. A variable delay with a mean of 0.5 sec. and fluctuating with a standard variation of 0.05 sec. is applied on the communication channel from Simulink. Fig. 5.45 shows the external forces for each actuated joint. The first joint of slave pantograph contacts with the environment between $t = 15$ sec. and $t = 40$ sec while the second joint contacts between $t = 15$ sec. and $t = 50$ sec. After $t = 50$ sec. the human and environmental forces are released from the robots however the position convergence can not be achieved this time. A significant steady state error is observed in Fig. 5.46.

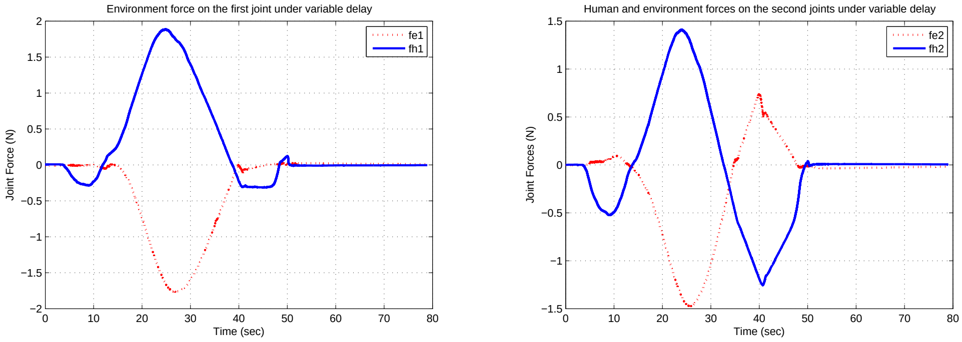

Figure 5.45: Joint Forces

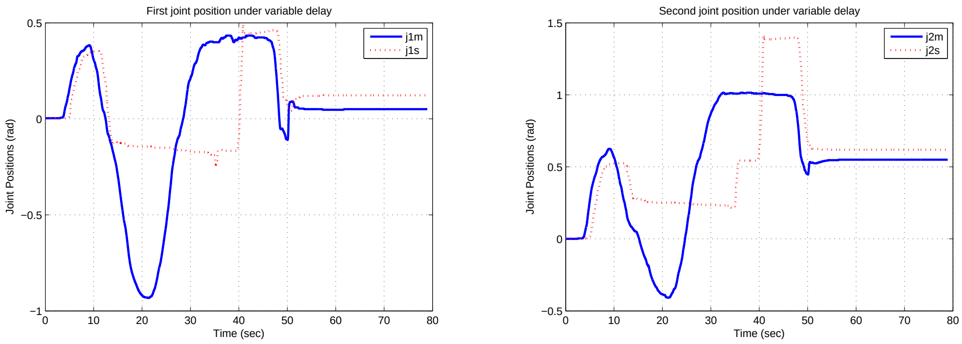

Figure 5.46: Joint Positions

Chapter VI

6 Concluding Remarks and Future Work

In this thesis, a novel observer based delay compensation method is proposed for the position control of a bilateral teleoperator system with nonlinear components. Delay compensation method is designed for bilateral systems consisting of nonlinear teleoperators since nonlinear robots are commonly used in many telerobotics applications to handle complex tasks. In this work not only nonlinear but also uncertain dynamics of the manipulators are linearized by a disturbance observer. A sliding observer is defined to predict the future states of the slave manipulator. This method takes place among the robust compensation techniques in the literature since the robustness of the system is increased with both disturbance observers and sliding mode control in the observer dynamics. Stable operation is guaranteed by simple PD type controllers which use the predicted states as feedback signals.

The performance of the proposed method is demonstrated with simulations and experiments performed on different nonlinear plants (scara robot and pantograph robot) considering constant and variable communication delays. For both of the delay types the simulation results show that the position tracking performance is successful. Predictor observer yields the convergence of the estimated states to the future of the actual states of the slave system. Thus, the control signal generated at the master side is able to control the slave robot successfully. Similar results are obtained with experiments performed on a pair of pantograph robots.

The proposed delay compensation method which is designed and tested for free motion is improved for force reflecting teleoperation where transperancy is the main concern. The well known four channel control architecture is modified in the observer based control framework as three channel architecture. Control efforts for both of the master and slave manipulators are calculated at the master side by using master's position, slave's predicted position, estimated human and environment forces. It may be impossible to reach the remote system therefore designing the control signals in master side allows us to make any modifications on control calculations immediately in any unexpected situations. The method is tested in simulations and experiments. Simulations are carried out on nonlinear robots (scara, pantograph) and experiments are performed on 1 DOF linear robots. The results was satisfactory but the experiments should be carried out on pantographs as nonlinear plants.

A number of different types of disturbance observes which are basically low-pass filters are used in the system. Since using low pass filter creates delay, this increases the phase lag resulting by the communication delay. The filter generated delay can be decreased with a proper tuning of cut-off frequency of the filters. Decreasing the cut-off frequency decreases the phase lag, however as the cut off frequency is decreased the performance of the filter degrades as disturbances with high frequencies are not estimated. Similarly since the external forces are estimated by a kind of disturbance observer, increasing the cut off frequency provides a better estimation. Therefore it can be concluded that the performance of the method is highly dependent on the number of the observers and their cut-off frequency values.

In the experiments the communication delay is introduced virtually from Matlab/Simulink. For more realistic implementations, a network communication should be established between the master and slave systems.

References

[1] T. B. Sheridan, W. R. Ferrell , "Remote Manipulative Control with Transmission Delay", IEEE Transactions on Human Factors in Electronics, 4, 25-29, 1963.

[2] W. R. Ferrell, "Remote manipulation with transmission delay", IEEE Transactions on Human Factors in Electronics", 6, 24-32, 1965.

[3] W.R.Ferrell, "Delayed force feedback, IEEE Transactions on Human Factors in Electronics", 449-455, October 1966.

[4] G. M. H. Leung, B. A. Francis and J. Apkarian, "Bilateral Ccontroller for Teleoperators with Time Delay via mu-Synthesis, IEEE Trans. on Robotics and Automation, Vol. 11, No. 1, pp. 105-116, Feb. 1995.

[5] R. Lin and T. Namerikawa, "Robust Control of Master-Slave Robot System Considering Environmental Uncertainties", Proc. of the IEEE/ASME Int. Conf. on AIM 2005, pp. 1299-1304, 2005.

[6] R. J. Anderson and M. W. Spong, "Bilateral Control of Teleoperators with Time Delay", in Proceedings IEEE Conference on Decision and Control, pp. 167-173, 1988.

[7] R. J. Anderson and M. W. Spong, "Asymptotic stability for force reflecting teleoperators with time delay", IEEE Trans. Autumat. Contr., pp. 1618-1625, 1989.

[8] J. E. Colgate, "Power and impedance scaling in bilateral telemanipulation", Procedings of the 1991 IEEE International Conference on Robotics and Autmation, Sacramento, California, April 1991.

[9] K. Kosuge, T. Itah, T. Fukuda, "Scaled telemanipulation with communication time delay", Proceedings of the 1996 IEEE International Conference on Robotics and Automation, Minneapolis, Minnesota, April 1996.

[10] G. Niemeyer, J. J. E. Slotine, "Stable Adaptive Teleoperation", IEEE Journal of Oceanic Engineering, Vol. 16, No. 1, pp. 152-162. Jan. 1992.

[11] G. Niemeyer, J. J. E. Slotine, "Transient Shaping In Force-Reflecting Teleoperation", In Proc. Int. Conf. on Advanced Robotics, Vol. 1, pp. 261-266, June 1991 IEEE

[12] S. Hirche and M. Buss, "Telepresence control in packet switched communication networks", Proceedings of the 2004 IEEE International Conference on Control Applications Taipei, Taiwan, September 2-4, 2004.

[13] R. Oboe and P. Fiorini, "Internet-Based Telerobotics: Problems and Approaches, International Conference of Advanced robotics (ICAR 97)", Monterey, CA, USA, 1997.

[14] R. Oboe and P. Fiorini, "Issues on internet based teleoperation", in Proc. Syroco'97, Nantes, France, Sept. 1997, pp. 611-617.

[15] R. Oboe and P. Fiorini, "A Design and Control Environment for Internet-Based Telerobotics", The International Journal of Robotics Research, vol. 17, pp. 433-449, April 1998.

[16] R. Lozano, N. Chopra, and M. Spong, "Passivation of force reflecting bilateral teleoperators with time varying delay", Proceedings of Mechatronics 02, Entschede, The Netherlands, pp. 24-26, 2002

[17] N. Chopra, M. Spong, S. Hirche and M. Buss, "Bilateral teleoperation over the Internet: the time varying delay problem", Proceedings of the American Control Conference, vol. 1, pp. 155-160, 2003.

[18] G. Niemeyer, J. J. E. Slotine, "Towards Force Reflecting Teleoperation Over the Internet", International Conference on Robotics and Automation, May 1998.

[19] N. Chopra, P. Berestesky, M. W. Spong, "Bilateral Teleoperation Over Unreliable Communication Networks", IEEE Transactions on Control Systems Techology, 2008.

[20] C. Benedetti, M. Franchini, P. Fiorini, "Stable tracking in variable time-delay teleoperation", In Proceedings of the 2001 IEEE/RSJ, International Conference on Intelligent Robots and Systems, Maui, Hawaii, USA, pp. 2252-2257, November 2001.

[21] N. Chopra, M. Spong, " On Position Tracking in Bilateral Teleoperation", Proceedings of the American Control Conference, vol. 6, pp. 5244-5249, 2004.

[22] N. Chopra, M. Spong, R. Ortega, and N. Barbanov, "On tracking preformance in bilateral teleoperation", IEEE Trans. Robot., vol. 22, no. 4, pp. 844-847, Aug. 2006.

[23] S. Munir and W. Book, "Control techniques and programming issues for time delayed internet based teleoperation", Journal of Dynamic Systems, Measurement, and Control, vol. 125, is. 2, pp. 157-277, 2003.

[24] T. Namerikawa and H. Kawada, "Symmetric Impedance Matched Teleoperation with Position Tracking," In proc. of 45th IEEE Conference on Decision and Control, pp. 4496-4501, 2006.

[25] D. J. Lee and, M. W. Spong, "Passive bilateral control of teleoperators under constant time delay," In Proc. IFAC World Congr., 2005.

[26] D. J. Lee and M.W. Spong. "Passive bilateral teleoperation with constant time delay. Robotics", IEEE Transactions on, Vol. 22, No. 2, pp. 269-281, April 2006.

[27] E. Nuño, R. Ortega, N. Barabanov, and L. Basañez, "A globally stable PD controller for bilateral teleoperators", IEEE Transactions on Robotics, Vol. 23, No. 3, pp. 753-758, 2008.

[28] E. Nuño, L. Basañez, R. Ortega, and Mark W. Spong , "Position tracking for nonlinear teleoperators with variable time delay", Int. J. Robotics Research, Vol. 28, No. 7, pp. 895-910, 2009.

[29] C. Andriot, R. Foumier, and J. Vuillemey, "On the bilateral control of teleoperators with flexible joints and time delay by the passive approach", In Proc. 5th Int. Con Advanced Robotics, pp. 231-236, 1991.

[30] H. Kazerooni, T. I. Tsay, K. Hollerbach, "A controller design framework for telerobotic systems", IEEE Trans. Contr. Syst. Tech., Vol. 1, No. 1, pp. 50-62, March 1993.

[31] T.I. Tsay and H. Kazerooni, "A design framework for telerobotics using the H_∞ approach", In Proc. Am. Contr. Con, pp. 2931-2935, 1992.

[32] A. Sano, H. Fujimoto, M. Tanaka, "Gain-secheduled compensation for time delay of bilateral teleoperation systems", Proceedings of the IEEE International Conference on Robotics and Automation, pp. 1916 - 1923, 1998.

[33] J. Kikuchi, K. Tekeo, K. Kosuge, "Teleoperation system via computer network for dynamic environment", Proc. IEEE Int. Conf. on Robotics and Automation, pp. 3534-3539, 1998

[34] J.H. Park, H.C. Cho, "Sliding mode controller for bilateral teleoperation with varying time delay", In Proc. IEEE Int. Conf. on Advanced Intelligent Mechatronics, pp. 311-316, September 1999.

[35] O. J. M. Smith, "A Controller to overcome dead time", ISA. Journal, Vol. 6, No. 2, pp. 28-33, 1959.

[36] H. Arioui, S. Mammar and T. Hamel, "A Smith prediction based Haptic Feedback Controller for Time Delayed virtual Environments Systems", American Control Conference, pp. 4303-4308, May 2002.

[37] S. Munir, W. J. Book, "Wave-Based Teleoperation with Prediction", Proceedings of the American Control. Conference, pp. 4605-461 , June 2001.

[38] S. Munir and W. Book, "Internet-based teleoperation using wave variables with prediction", IEEE/ASME Transactions on Mechatronics, Vol. 7, No. 2, pp. 124-133, June 2002.

[39] S. Ganjefar, H. Momeni, and F. Janabi-Sharifi, "Teleoperation Systems Design Using Augmented Wave-Variables and Smith Predictor Method

for Reducing Time-Delay Effects", Proc. IEEE Int. Symp. Intelligent Control, pp. 333-338, Oct. 2002

[40] A. C. Smith, K. H. Zaad, "Smith Predictor Type Control Architectures for Time Delayed Teleoperation", International Journal of Robotics Research, Vol. 25, No. 8, pp. 797-818, 2006.

[41] K.Natori, T.Tsuji, K.Ohnishi, A.Hace, K.Jezernik, "Robust Bilateral Control with Internet Communication," Proceedings of the 30th Annual Conference of the IEEE Industrial Electronics Society, Busan, Korea, Vol. 3, pp.2321-23262, 6 November 2004.

[42] K.Natori, R. Oboe, K.Ohnishi , "Analysis and Design of Time Delayed Control systems with Communication Disturbance Observer", In Proceedings of the IEEE international symposium on industrial electronics, Vigo, Spain, pp. 3132-3137, 2007

[43] K.Natori, T.Tsuji, K.Ohnishi, "Time Delay Compensation by Communication Disturbance Observer in Bilateral Teleoperation Systems," Proceedings of The IEEE 9th International Workshop on Advanced Motion Control , Istanbul, Turkey, pp. 218-223, 27-29th March 2006.

[44] W. Iida, K. Ohnishi, "Reproducibility and Operationality in Bilateral Teleoperation", Proceedings of the 8th IEEE International Workshop on Advanced Motion Control, AMC'04-KAWASAKI, pp. 217-222, March, 2004.

[45] N. Iiyama,K.Natori, K.Ohnishi, "Bilateral Teleoperation Under Time-Varying Communication Time Delay Considering Contact with Envi-

ronment, Electronics and Communications in Japan, Vol. 92, No. 7, 2009

[46] A A Rahman, K. Natori, K. Ohnishi, "Disturbance Decomposition of Time Delay System by shadow Robot Based on Network Disturbance Concept, IEEE International Conference on Digital Object Identifier, pp. 1-6, Industrial Technology ICIT 2009, 2009.

[47] T. Murakami, F. Yu, and K. Ohnishi, "Torque sensorless control in multi degree-of-freedom manipulator", IEEE Transactions on Industrial Electronics, Vol. 40, No. 2, pp. 259-265, April,1993.

[48] D. A. Lawrence, "Stability and transparency in bilateral teleoperation", IEEE Transactions on Robotics and Automation, vol. 9, no. 5, pp. 624-637, October 1993

[49] Y. Yokokohji, T. Yoshikawa, "Bilateral control of master slave manipulators for ideal kinesthetic coupling formulation and experiment", IEEE Transactions on Robotics and Automation, Vol. 10, No. 5, pp. 605-620, 1994.

[50] P. F. Hokayem and M. W. "Spong Bilateral Teleoperation: An historical survey", Automatica, vol. 42, pp. 2035-2057, 2006.

[51] M. Zhu, S. E. Salcudean, "Achieving transparency for teleoperator systems under position and rate control", In Proceedings of the IEEE/RSJ international conference on intelligent robots and systems, Vol. 2, pp. 7-12, 1995.

[52] K. Hashtrudi-Zaad and S. E. Salcudean, "Adaptive Transparent Impedance Reflecting Teleoperation", Proceedings of the IEEE Inter-

national Conference on Robotics and Automation, Minneapolis, Minnesota, pp. 1369-1374, April 1996.

[53] K.Hashtrudi-Zaad and S.E.Salcudean, “On the Use of Local Force Feedback for Transparent Teleoperation”, Proceedings of the 1999 IEEE International Conference on Robotics and Automation, pp.1863 1869, May 1999

[54] W. H. Zhu, S. E. Salcudean, “Teleoperation with Adaptive Motion/Force Control”, IEEE International Conference on Robotics and Automation, pp.231-237, Detroit, MI, May 1999.

[55] G. Niemeyer, J.E. Slotine, “Using Wave variables for System Analysis and. Robot Control”, IEEE Trans., pp. 1619-1625, 1997

[56] G. Niemeyer, J.J.E. Slotine, “Designing Force Reflecting Teleoperation with Large Time Delays to Appear as Virtual Tools, Proc. of the IEEE ICRA 1997 Vol. 3, pp. 2212-2218,1997.

[57] K. Kawashima, K. Tadano, G. Sankaranarayanan and B. Hannaford, “Bilateral Teleoperation with Time Delay using Modified Wave Variables”, 2008 IEEE/RSJ International Conference on Intelligent Robots and Systems Acropolis Convention Center Nice, France, Sept, 22-26, 2008

[58] J.H. Park, H.C. Cho, “Sliding mode controller for bilateral teleoperation with varying time delay”, In Proc. IEEE Int. Conf. on Advanced Intelligent Mechatronics, pp. 311 316, 1999.

[59] T. Leblebici, B. Çallı, M. Unel, A. Sabanovic, S. Bogosyan, M. Gokasan, “Delay Compensation in Bilateral Control Using Predictor Sliding Mode

Observers", Turkish Journal of Electrical Engineering and Computer Sciences (TJEECS), December 2011.

[60] S. Dikyar, T. Leblebici, D. Ozcelik, M. Unel, A. Sabanovic, S. Bogosyan, "Delay Compensation for Nonlinear Teleoperators Using Predictor Observers", IEEE International Conference on Industrial Electronics, Control, and Instrumentation (IECON 2010), November 7-10, Glendale, AZ, USA, 2010.

[61] T. Leblebici, S. Dikyar, D. Ozcelik, M. Unel, A. Sabanovic , "Doğrusal Olmayan İki Yönlü Denetim Sistemlerinde Gözlemci Tabanlı Zaman Gecikme Telafisi", TOK.10: Otomatik Kontrol Ulusal Toplantısı, 21-23 , Gebze Yüksek Teknoloji Enstitüsü, Kocaeli, Turkey, Eylül 2010.

[62] B. Çallı, T. Leblebici, M. Unel, A. Sabanovic, S. Bogosyan, M. Gokasan , "İki Yönlü Denetimde İletişim Kanalındaki Gecikmenin Kayan Kipli Gözlemci Kullanarak Telafisi", TOK.09: Otomatik Kontrol Ulusal Toplantısı, İstanbul Teknik Üniversitesi, İstanbul, Turkey, 13-16 Ekim 2009.

[63] J. Yan and S. E. Salcudean, "Teleoperation controller design using H-infinity optimization with application to motion-scaling", IEEE Trans. Contr. Syst. Technol., vol. 4, pp. 244-258, May 1996

[64] K. Hashtrudi-Zaad and S.E. Salcudean, "On the Use of Local Force Feedback for Transparent Teleoperation", In Proceedings of the IEEE International Conference on Robotics and Automation, pp. 1863-1869, Detroit (MI), US, 1999.

[65] K. Hashtrudi-Zaad and S.E. Salcudean, "Analysis of Control Architectures for Teleoperation Systems with Impedance/Admittance Master and Slave Manipulators", International Journal of Robotics Research, Vol. 20, No. 6, pp. 419-445, 2001.

[66] O. J. M. Smith, "Posicast control of damped oscillatory systems", In Proceedings of the IRE, Vol. 45, pp. 1249-1255, 1957.

[67] K. Ohnishi and T. Murakami, "Advanced Motion Control in Robotics", IEEE IECON, vol. 2, pp. 356-359, 1989.

[68] K.S. Eom, I.H. Suh, W.K. Chung, S.R. Oh, "Disturbance observer based force control of robot manipulator without force sensor", In Proc. 1998 IEEE Int. Conf. Robot. Autom, vol. 4, pp. 1916-1923, 1998.

[69] H. Yu, "Modeling and control of hybrid machine systems−a five−bar mechanism case", International Journal of Automation and Computing, pp. 235-243, 2006.

[70] K. Erbatur and B. Çallı, "Fuzzy boundary layer tuning as applied to the control of a direct drive robot", The 33rd Annual Conference of the IEEE Industrial Electronics Society, Taipei, IEEE, November 2007